Design, construction and characterization of LysK endolysin display phage against *Staphylococcus aureus*

by

Farah El-Zarkout

A thesis

presented to the University of Waterloo

in fulfillment of the

thesis requirement for the degree of

Master of Science

in

Pharmacy

Waterloo, Ontario, Canada, 2013

Author's Declaration

I hereby declare that I am the sole author of this thesis. This is a true copy of the thesis, including any required final revisions, as accepted by my examiners.

I understand that my thesis may be made electronically available to the public.

Abstract

The growing threat of drug- resistant *Staphylococcus aureus* (*S. aureus*) infections mandates the need to develop novel, effective and alternative antibacterial therapeutics. Despite infection prevention and control measures, methicillin resistant *S. aureus* (MRSA)-associated deaths reached 11,285 in 2011 in the USA (CDC, 2013). To counteract the threat of drug resistant *S. aureus,* we sought to construct and characterize a novel therapeutic based on the display of lytic antibacterial enzymes, termed endolysins. These endolysins were displayed on the surface of a specific bacterial virus, bacteriophage (phage), to generate lytic antibacterial nanoparticles. Endolysins are encoded individually by a variety of double-stranded DNA phage and act to direct host lysis and escape. These lytic enzymes confer a high degree of host specificity that could potentially substitute for, or be combined with, antibiotics in the treatment of gram-positive drug resistant bacterial infections such as MRSA.

In this study, modular domains of the phage-encoded endolysin K enzyme, specific to *S. aureus*, were displayed on the capsid surface of phage lambda (λ) *via* fusion with the λ major head (capsid) protein, gpD. The constructs of displayed endolysins were prepared in various combinations to maximize the functional display of gpD::X fusions on the phage. Phage lysates were generated, collected and purified and lysis was investigated by adding to fresh lawns of MRSA, vancomycin resistant *S. aureus* (VRSA) and bovine *S. aureus*. Phage preparations did not readily confer cell lysis, likely due to poor incorporation of

the fusions onto the functional phage capsid. We purified the fusion proteins (gpD::X) and tested them for their lytic activity. We noted that the activity of the gpD::LysK protein was not impaired by the fusion and demonstrated lysis on live and dead (autoclaved) bovine *S. aureus*. In contrast to gpD::LysK, the gpD::CHAP protein fusion, expressing only the CHAP catalytic domain of endolysin K showed variable results in the lysis assays that we performed. In the zymogram assay, gpD::CHAP did not elicit any observable lysis on live bovine *S. aureus* cells, but did effectively lyse dead cells of the same *S. aureus* species; however, it was highly lytic in the inhibition assay on bovine *S. aureus*. The CHAP::gpD protein fusion, which is the CHAP domain fused to the N terminus of gpD only showed its ability to inhibit bovine *S. aureus* growth on the inhibition assay.

The fusion of endolysin K or its CHAP domain to gpD protein does not seem to interfere with lytic activity, but may result in recalcitrant gpD fusions that compromise the ability to efficiently decorate the phage capsid. Suggestions for improved fusion capsid integration are discussed.

Acknowledgements

{But perhaps you hate a thing and it is good for you; and perhaps you love a thing and it is bad for you. And Allah Knows, while you know not.}

(Surah Albaqarah, 216)

My sincerest gratitude goes to Allah (swt). He has given me the strength, patience and hope that I needed to go through my graduate studies.

I would like to express my outmost appreciation to my supervisor, Dr. Roderick Slavcev for giving me the opportunity to do my graduate studies in his laboratory. I would not be where I am now if it were not for his continuous support and guidance.

I would like to also thank my parents, Aref and Hiam El-zarkout, my brothers, fadi and Hadi for their endless love and support. My gratitude also goes to my relatives in Canada and back home in Lebanon for believing in me.

A lot of sincere appreciation goes to my best friend, O.G., for being there and giving me a hand throughout my masters. My two years of graduate studies would not have been the same without you. I'm endlessly grateful.

I believe I caused some headaches to a lot of girl friends for coming to them in my moody and stressful times and I'm convinced that my MSc. experience would not

have been same if they were not around. Naheda, Azita, Heba, Lubna, Aula, Nafiseh, Jessica and Nadia.

Thank you to my colleagues, Tarek, Ren, and Dr. Olla, at school of pharmacy for being there to help me whenever I needed assistance.

I'm also grateful for working with several bright undergraduate students, Peggy Lam, Marie Chan, Adriana Too, Natalle Chan, Dip Shah, Judy Chong your assistance and cooperation was a tremendous help. I'm glad that I got to work with amazing individuals like you.

Last but not least, I would like to thank Dr. Blay for his feedback and guidance on my project and for seeing the leader and scientist in me.

Dedication

I dedicate this work to everyone who believes in me and to everyone who believes that dreams do come true, but only with hard work and positive outlook.

Table of Contents

List of Figures

List of Tables

List of Abbreviations and Glossary

Ap: Ampicillin is used as a selectable marker in media to isolate ampicillin-resistant bacterial strains.

BHI: Brain Heart Infusion is a very rich growth media used for culturing *S. aureus* strains.

Cm: Chloramphenicol is used as a selectable marker in media to isolate chloramphenicol-resistant bacterial strains.

CHAP: Cysteine and histidine-dependent amino hydrolase domain, a catalytic domain of phage K endolysin, LysK.

CFU: Colony forming units estimate the number of cell particles present in one unit volume based on the potential colony that is generated by each cell when immobilized on a solid agar medium.

dsDNA: double stranded DNA.

EDTA: ethylene-diamine-tetraacetic acid chelates divalent cations.

Episomal DNA: Extrachromosomal DNA that is an autonomous replicon.

EOP: Efficiency of plating is a relative efficiency measure of virus ability to plate under experimental conditions.

EtBr: Ethidium Bromide is a nucleic acid fluorescent tag used to visualize nucleic acid under ultra violet (UV) light.

eGFP: efficient green fluorescent protein possesses a chromophore that emits green fluorescent light under the blue-violet light range. It is linked to proteins of interest for visual tracking and analysis.

gpD (gene product D): The major capsid protein encoded by the phage λ *D* gene. The gpD protein tolerates translational fusions to the N or C termini and forms the basis for λ-mediated lytic phage display.

His-tag: A short peptide tag that consists of at least six histidine amino acids. It is usually incorporated in protein sequences and used to bind to cations (Nickel) for efficient protein purification.

Kn: Kanamycin is an antibiotic used as a selectable marker in media to isolate kanamycin-resistant bacterial strains.

LB: Luria Bertani is a standard rich growth medium used for cell culturing.

mecA: An acquired foreign gene by *S. aureus* that confers a methicillin- resistant phenotype.

MRSA: methicillin-resistant *S. aureus*. *S. aureus* strains that are resistant to methicillin and its derivatives.

MDRSA: Multi-drug resistant *S. aureus*. *S. aureus* strains that are resistant to methicillin, vancomycin and other antibiotics.

MCS: multiple cloning site - DNA sequences on cloning vectors that contain a variety of restriction enzyme recognition sequences.

PEG: Polyethelene glycol is a cyclic ether polymer that was used here to bind and precipitate phage particles.

PBP: Penicillin binding protein is involved in peptidoglycan synthesis and the target for beta-lactam antibiotics.

PFU: Plaque forming units estimate the number of viral particles forming plaques in one unit volume based on the ability of one phage particle to generate a visible plaque when immobilized on solid agar medium.

SH3: SRC Homology 3 domain, a specificity domain of phage K endolysin K.

SDS: Sodium Deodycl Sulfate- used to denature proteins in protein gels.

SDS: PAGE- Sodium Deodycl Sulfate Polyacrelamide Gel Electrophoresis, the electrophoresis gel for proteins.

SPA- calmodulin-binding- 3X FLAG tag

VISA: Vancomycin intermediate *S. aureus* strains that display intermediate susceptibility to vancomycin.

VRSA: Vancomycin resistant *S. aureus*. *S. aureus* strains that display resistance to vancomycin.

Chapter 1: Literature Review

Staphylococcus aureus

S. aureus is a Gram-positive bacterium that possesses a thick outer peptidoglycan layer and lacks the outer membrane possessed by its Gram-negative counterparts (Szweda et al., 2012). This murein layer (Figure 1) is comprised of amino sugars termed N-acetylglucosamine and N-acetylmuramic acids that make up the glycan chains and teichoic acids that function as peptidoglycan cross-linking regulators or protein recognition and binding sites; on the surface, they may serve as pathogenic epitopes, ligands or environment communicators (Szweda et al., 2012; Navarre and Schneewind, 1999).

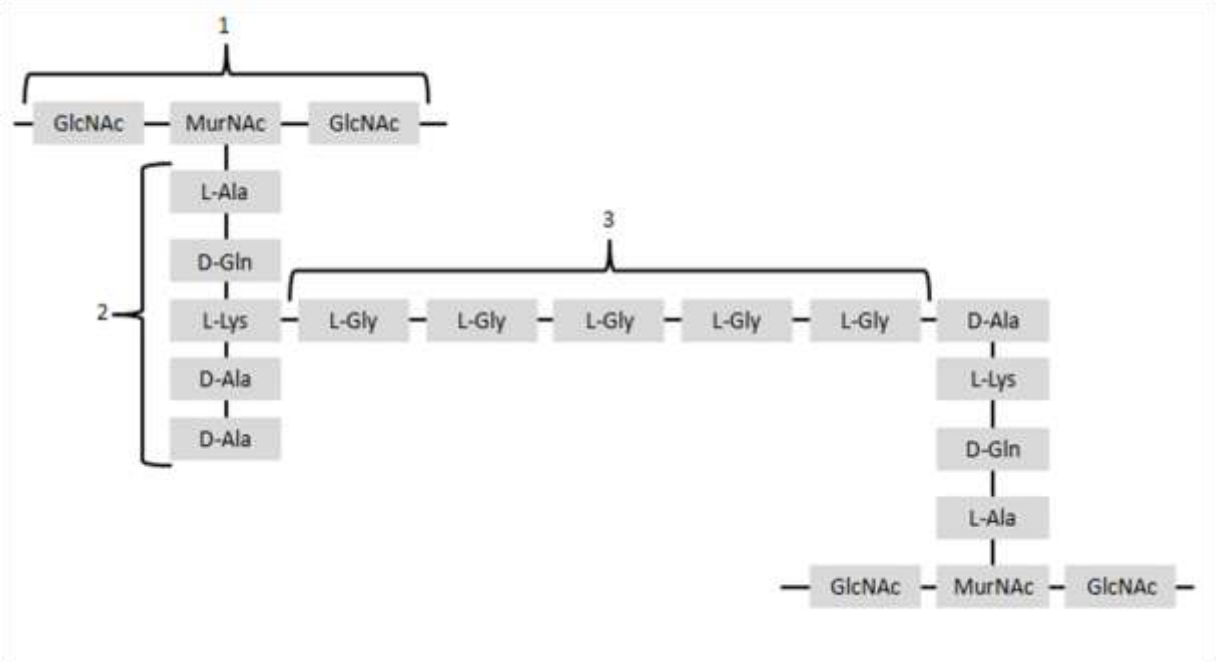

Figure 1. Peptidoglycan Units. The peptidoglycan is made up of several different units of sugars and amino acids. Five units of L-Gly (3) act as a cross bridge between peptide bonds (2) branching off the amino sugars (1).

S. aureus is a commensal microorganism that naturally inhabits the skin, nares and internal membranes of humans and animals without eliciting any harmful effects under normal conditions (Kluytmans et al., 1997; Lowy, 1998). The bacterium is known to colonize 30-50% of healthy adults where 10-20% of the colonized individuals demonstrate persistent colonization (Lowy, 1998). However, the bacterium is likely to impart infections in healthy individuals and can be particularly detrimental for immunocompromised individuals. In Canada, *S. aureus*-mediated infections ranked first among other pathogenic bacterial strains in 2011, with a prevalence of 18.2% (Canadian Antimicrobial Resistance Alliance, 2011).

Staphylococcal-mediated diseases vary from acute infections of the skin, to chronic and/or systemic infections upon entrance into the blood, bones and lungs (Kiedrowski & Horswill, 2011). The lethal diseases associated with staphylococcal infections include sepsis, endocarditis, and toxic shock syndrome (Lowy, 1998). In addition, *S. aureus* develops a complicated and stronger pathogenicity with the acquisition and development of resistance to antibiotics. Drug resistance is driven by its strong predisposition to mutagenesis and the acquisition of resistance genes by horizontal gene transfer. This has resulted in the isolation of several strains capable to resist one or a combination of antibiotics—methicillin resistant *S. aureus* (MRSA), vancomycin resistant *S. aureus* (VRSA) and multiple drug resistant *S. aureus* (MDRSA) (Lowy, 1998). The first celbenin (methicillin)-resistant *S. aureus* strain was identified and isolated in 1961 (Knox, 1961) and its burden on hospital acquired infections is

noteworthy. Most recent data show that MRSA infections represent 4.3% of total infections among other non-drug resistant bacterial strains in Canada, indicating that they impose a severe threat (Canadian Antimicrobial Resistance Alliance, 2011).

In order to understand the mechanisms behind *S. aureus* drug resistance it is important to first understand the processes of various antibiotics and their antibacterial properties. Beta-lactams, aminoglycosides, macrolides, tetracyclines and glycopeptides antibiotics lyse or inhibit growth of antibiotic-susceptible staphylococcal cells by interfering with peptidoglycan synthesis or other cell survival mechanisms. Peptidoglycan synthesis is inhibited by penicillin and its derivatives that recognize and bind to the cytoplasmic penicillin-binding protein (PBP), thereby inhibiting the binding of D-alanine (monomers used in peptidoglycan chain precursors) to existing pentaglycine chains (Figure 1; chains 2 &3) (Hiramatsu, 1998). Other antibiotics including aminoglycosides, macrolides and tetracyclines inhibit the vital process of protein synthesis by binding to the cytoplasmic ribosomes of the bacterium (Hiramatsu, 1998). Alternatively, glycopeptides including vancomycin and teicoplanin inhibit transglycosylation in *S. aureus* by binding to the termini of the newly formed D-alanyl-D-alanine peptides (Hiramatsu, 1998; Hiramatsu, 2001).

Prior to the discovery of antibiotics, approximately 80% of *S. aureus* infections were deemed fatal (Skinner & Keefer, 1941) and susceptible *S. aureus* strains developed resistance to penicillin only two years after its discovery in 1940 (Lowy, 2003). The insusceptibility of isolated *S. aureus* strains to penicillin has

led to the discovery and introduction of methicillin in 1961. However, shortly after its introduction, resistant cases of methicillin-resistant *S. aureus* were also discovered (Lowy, 2003). *S. aureus* acquired resistance to beta-lactams through the incorporation of the foreign *mecA* gene that encodes a mutated PBP, termed PBP2' into its genome (Hartman and Tomasz, 1984; Ito et al., 1999). PBP2' exhibits low binding affinity for beta-lactams and renders peptidoglycan synthesis insensitive to the added methicillin in MRSA samples (Hartman and Tomasz, 1984).

Following the emergence of MRSA strains (Ruef, 2004) vancomycin became the last resort for antibiotic treatment modality. However, the extensive usage of vancomycin has since led to either reduced or complete loss of vancomycin susceptibility of *S. aureus* strains, termed Vancomycin Intermediate *S. aureus* (VISA) (Ruef, 2004) and vancomycin resistant *S. aureus* (VRSA), respectively. VISA was first identified from a clinical specimen in Japan in 1997 (Chang et al., 2003), whereas the first complete VRSA strain was identified five years later in the US (Weigel, 2003). Some isolates of VRSA were also resistant to beta-lactam antibiotics, thus making these isolates multi drug resistant (Weigel, 2003). Intermediate *S. aureus* strains were since identified to harbour mutations in several regulatory loci: *walRK, clpP, graRS, and vraSR* genes (Shoji et al., 2011). *graRS* and *vraSR* genes encode cell wall synthesis regulatory proteins that confer vancomycin intermediate resistance in Mu50 VRSA strains (Hiramatsu, 2001; Cui et al., 2000). Mutations in *walRK, clpP, graRS, and vraSR* genes upregulate the synthesis of the peptidoglycan to produce an

abnormally thick cell wall, thereby hindering effective vancomycin penetration into the cell (Hiramatsu, 2001). Genetic studies of VRSA have also revealed foreign genetic material encoding the *vanA* gene that is responsible for the mutation from D-alanyl-D-alanine to D-alanyl-D-lactate chain, thereby rendering vancomycin ineffective against the mutated disaccharide (Weigel, 2003).

The treatment costs of *S. aureus* infections vary based on the drug susceptibility of the infecting strain, rising significantly with reduced drug susceptibility. For instance, in the US, where a 6 months treatment regimen for methicillin-sensitive *S. aureus* infection may cost approximately $16,000, an otherwise identical MRSA infection treatment would be more than double this cost at about $36,000 (Filice et al., 2010). In addition to the increase in treatment costs, antimicrobial resistance has led to prolonged hospital stays and an increase in morbidity and mortality rates. There are currently very few antibacterials present in the market for a number of common antibiotic resistant strains (Infectious Diseases Society of America Report, 2004). As some strains could be resistant to multiple common antibiotics, there are few therapeutic options left to treat these multidrug resistant infections, and those that are available tend to be expensive, toxic to the patient and less effective in treatment (Center for Disease Prevention and Control, 2013). In conclusion, the threat of antimicrobial resistance is very high and there is strong and urgent need to develop novel antibacterial agents.

Lysins as Antibacterial agents

As the treatment of microbial infections proves to be increasingly difficult with the increasing incidence of antibiotic-resistant strains (Lowy et al., 2003), a promising alternative antibacterial strategy includes the exploitation of phage and phage-encoded enzymes in the development of novel antibacterial therapeutics. Enzymes that hydrolyze the peptidoglycan layer of their bacterial host are termed lysins, and they are gaining worldwide attention as naturally occurring, exploitable antibacterials (Rodríguez-Rubio et al., 2012; Szweda et al., 2012). From these peptidoglycan hydrolases, a class of highly lytic lysins encoded by phage are encoded and naturally expressed by dsDNA phage as a means of host escape at the end of their infectious cycles (Borysowski et al., 2006; Loessner, 2005). The first discovered lysins were virolysin and phage associated lysins (PAL), which were found to be secreted from phage-infected, gram-positive *S. aureus* cells (Ralston et al., 1957, Sonstein et al., 1971). Although not all phage are "lytic" by classification, all known dsDNA phage are capable of a lytic lifecycle at the end of which, they must lyse the host cell in order to release new phage progeny. This lytic activity is controlled by the expression of two enzymes, holin and lysin (termed endolysin when phage-encoded), during the late gene expression period of the phage as a highly time-controlled process. During specific conditions such as high phage density, the holin, which is basically a monomer or a single subunit is proposed to assemble into pore-forming oligomers or multiple subunits in the cell membrane that in a precisely timed manner, depolarize the membrane. This depolarization event

then enables the endolysins to egress from the cytoplasm to the periplasm where they may hydrolyse their substrate target, the peptidoglycan layer, and lyse the cell (Sonstein et al., 1971; Ralston et al., 1957; Loessner, 2005).

Endolysins are categorized by their targeted peptidoglycan bond substrates and catalytic activity. Lysozymes, for example, are muramidases that act upon linked N-acetylglucosamine and N-acetlymuramic acid bonds. In contrast, endopeptidases catalyze peptide bonds and amidases hydrolyze amide bonds that link the sugars and peptides in the peptidoglycan layer (Fischetti, 2005; Loessner, 2005). The external application of endolysins to lyse bacteria is highly specific, but generally only effective in lysing Gram-positives due to the absence of outer membrane of the cell that in Gram-negatives protects against endolysin access to the peptidoglycan (Loessner et al., 2005). Endolysins offer promising antibacterial alternatives, particularly against antibiotic resistant strains, as they target different sites than antibiotics to confer cell lysis. Phage-based enzymes are proving effective in the treatment of infections in mucosal membranes and blood of animal models. Fischetti (2005) describes that the advantages of phage lytic enzymes over antibiotics are their high specificity in lysing the target cells without affecting the natural microflora. For instance lytic enzymes derived from *S. aureus* phage only lyse *S. aureus* strains (Szweda et al., 2012). Resistance to endolysins are less likely due to the co-existence of phage with their specific bacterial host as phage must co-evolve with their bacterial hosts to ensure their sustainability (Fischetti, 2005; Borysowski et al., 2006). Several endolysins also possess two catalytic domains that hydrolyze different bonds in

the cellular peptidoglycan, again reducing the incidence of resistance (Szweda et al., 2012). Finally, to enhance their therapeutic activity and to avoid the development of resistance, antibiotics may be also used in combinatorial strategies with endolysins to treat bacterial infections (Szweda et al., 2012). In a study by Schmelcher et al. (2012), LysK from phage K and Lysostaphin, a staphylococcal endopeptidase, functioned synergistically and effectively in clearing staphylococci infections in cattle.

Endolysin K: The fairly recently discovered endolysin K (LysK), isolated from *S. aureus* cells infected with phage K, was found to be highly effective in lysing live gram-positive staphylococci cells, including antibiotic resistant strains (O`Flaherty et al., 2005). LysK crude extract was found to be highly efficient in killing 99% of MRSA cells within an hour (O`Flaherty et al., 2005). In addition to MRSA, LysK was also effective in lysing vancomycin and teicoplanin-resistant *S. aureus* strains (O`Flaherty et al., 2005).

Sequence studies and protein deletion analysis have revealed that LysK, a 54 kDa protein encoded by two open reading frames, is comprised of three domains: 1) an N-terminus CHAP (cysteine and histidine-dependent amino hydrolase) domain; 2) a C-terminal SH3 (SRC Homology 3) domain; and 3) a central catalytic amidase-2 domain flanked by the N- and C- termini (O'Flaherty et al., 2004; Loessner et al., 2005; Horgan et al., 2009; Figure 2). From deletion studies, upon removing the amidase-2 and SH3 domains, the endopeptidase-encoding CHAP catalytic domain remained active in cleaving the bond between the D-alanine in the stem peptide and glycine in the cross bridge peptide, thus

degrading the layered peptidoglycan (Becker et al., 2009; Horgan et al., 2009; Figure 3). Amidase-2 was also observed to catalyze the bond between the N-acetylmuramic acid and L-alanine of the stem peptide in live staphylococci cells (Becker et al., 2009). In contrast, the C-terminal SH3 domain was found to serve solely as a specificity domain that binds the endolysin to its substrate via teichoic acids in the peptidoglycan (Becker et al., 2009; Loessner et al., 2005; Horgan et al., 2009).

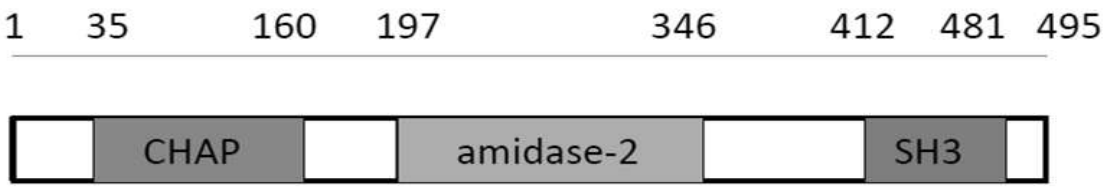

Figure 2. LysK domains.

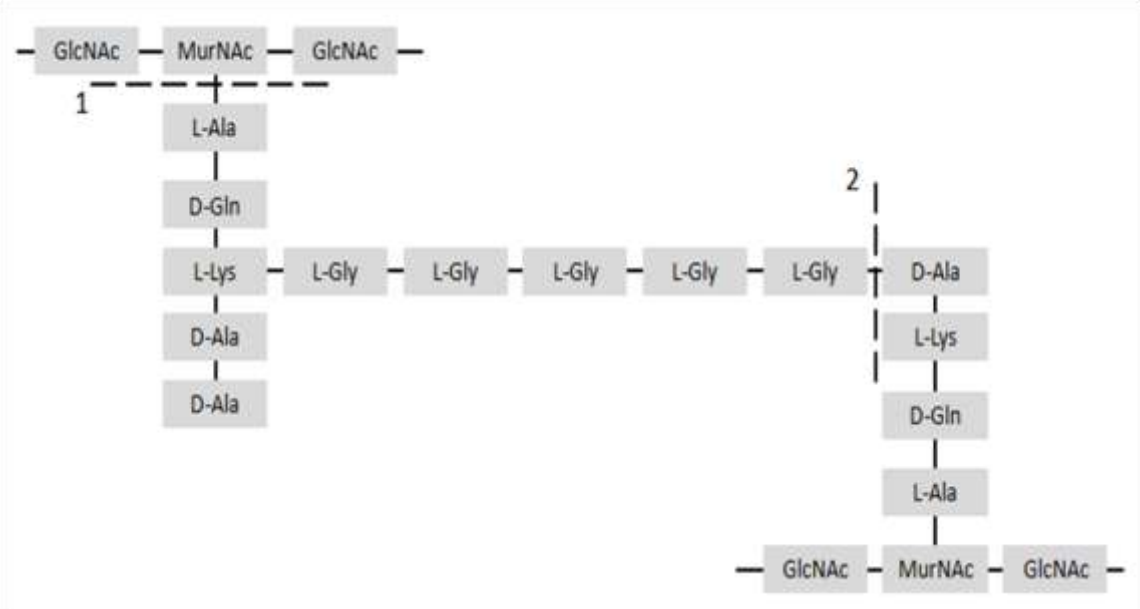

Figure 3. Peptidoglycan cut sites. Cut site 1 (dashed line) is recognized by amidase-2 of LysK, while cut site 2 (dashed line) is recognized by CHAP endopeptidase of LysK.

Currently, the only peptidoglycan hydrolase that is commercially available is the extensively studied Lysostaphin lysin which is native to *Staphylococcus simulans* (Becker et al., 2008), but can be used as a competitive defense mechanism against *S. aureus* (Schindler and Schuhardt, 1964). Lysostaphin is a peptidase that cleaves the bond between the glycine and alanine in *S. aureus* peptidoglycan (Browder et al., 1965). Since the identification of LysK as an endolysin with a wide virulent and drug resistant *S. aureus* host range (O'Flaherty et al., 2005), several studies have been performed to study LysK physiochemical properties. The biological stability of an enzyme being considered for antimicrobial applications is particularly important as stability directly affects the action of the enzyme. Low molecular weight additives such as glycerol or sucrose were found to increase LysK stability by 100 times (Filatova et al., 2010). The addition of such low weight molecular additives enable LysK to maintain 100% of its activity for up to a month at room

temperature, which is remarkable and very uncommon for most enzymes (Filatova et al., 2010). Other cofactors like the addition of divalent cations, Ca^{2+}, also increase LysK stability when added.

Several attributes of LysK potentiate its exploitation as a valuable and long-lived antibacterial in the treatment of *S. aureus*, including: 1) It can work in combination with antibiotics/other antimicrobials to clear infections; 2) It possesses two catalytic domains, which increase its catalytic activity and reduce likelihood of host resistance; 3) Its binding sites are highly conserved, further reducing the likelihood of bacterial resistance; and 4) Its activity may be enhanced by increasing its stability with low cost and abundant cofactors such as glycerol and calcium ions.

Phage display

The presentation of foreign functional peptides on phage surfaces is a process known as phage display and possesses a rich recent history of biotechnological applications (Bratkovic, 2009). Phage display is the process by which a foreign gene is fused to a structural phage gene that usually encodes a native resident protein on the phage surface. The translational fusion results in the co-expression of the foreign gene with the native resident phage gene (Bratkovic, 2009). Two types of phage have been extensively used to display foreign proteins.

Filamentous M13 and fd phage, which are non-lytic, were the first and most extensively employed phage to display proteins fused to their minor and major

coat proteins (III and VIII) (McCafferty et al., 1991; Fuh et al., 2000). However, there are several disadvantages and limitations to the filamentous phage system which include: 1) The exclusion of highly hydrophilic proteins/peptide fusions as the fused proteins must assemble in the hydrophobic inner membrane of the cell prior to phage assembly; 2) The exclusion of toxic protein fusions as filamentous phage infections are not lytic, but rather "bud" from the viable infected cell; and 3) The strong limitation on the low number of possible expressed fusions per phage (Bratkovic, 2009; Gupta et al., 2003).

In contrast, phage display systems offered by lytic dsDNA phage such as phage λ, T4, and T7, permit capsid assembly inside the host prior to cell lysis, thus eliminating the need for foreign proteins to cross the cell wall. In addition all three systems offer fusion potential in the order of several hundred per phage (Bratkovic, 2009).

The first documented use of λ in phage display was performed by Maruyama et al., (1994) who fused *E. coli* β-galactosidase and plant agglutinin fusions to the λ major tail protein, gpV. The gpV protein of 28.5 kDa, was truncated to a mutant protein of 18.8 kDa that lacks its C-terminal but still retained host infectivity (Casjens & Hendrix, 1974; Maruyama et al., 1994). Protein V, which is encoded by gene *V*, forms a hexamer of 32 copies in the noncontractile λ tail (Maruyama et al., 1994). Dunn (1995) displayed a target site for cyclic AMP (cAMP) on the C terminal of gpV, where the displayed cAMP site was recognized by the added kinase yielding in phosphorylation of the phage particles, indicating successful functional display of the target site. Despite the

successful exploitation of gpV for phage display, the display copy number was very limited and led to the eventual discovery and exploitation of the λ gpD display candidate.

The λ capsid is comprised of two major capsid proteins, gpE and gpD, encoded by λ genes *E* and *D*, respectively, and each with 405-420 copies per phage (Bratkovic, 2009; Casjens and Hendrix, 1974, Figure 4).

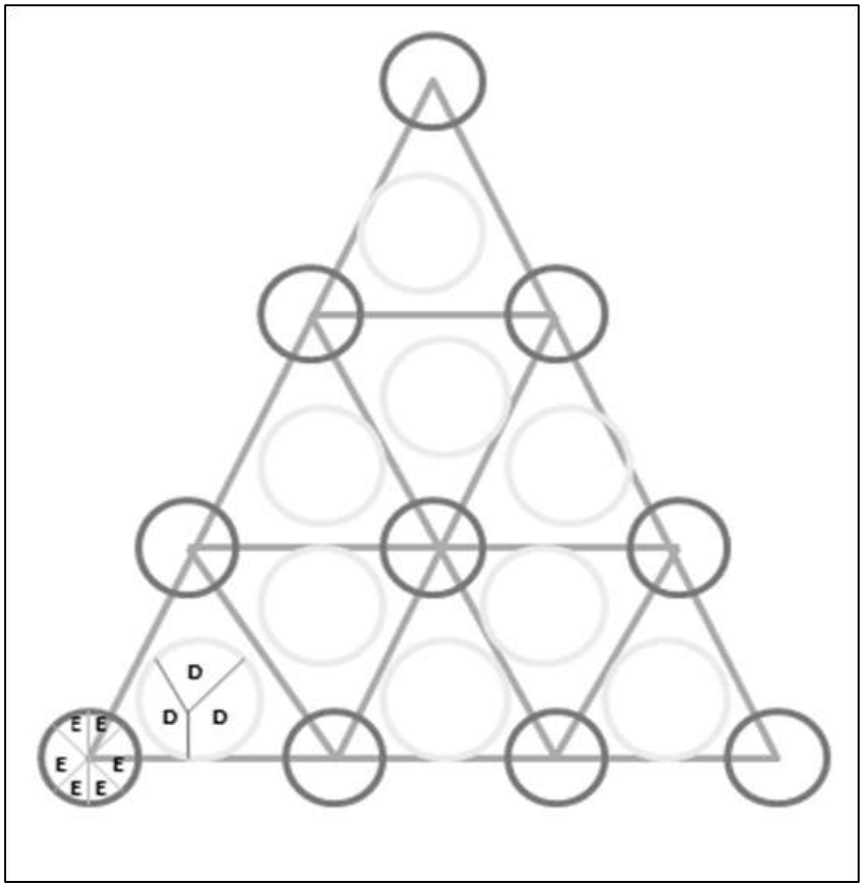

Figure 4. Phage λ capsid. The λ capsid is described as icosaherdal (20 faces) with a total of between 405-420 copies of the major capsid protein gpD. Protein gpD (yellow) forms trimers in the capsid surface, while gpE (blue) forms hexamers at roughly the same incorporation number per phage.

Protein gpD is 11.4 kDa in size and has a function in the assembly and stabilization of the phage prohead, initially formed by hexamers of gpE, upon the packaging of phage dsDNA (Sternberg and Hoess, 1995; Sternberg and Weisberg, 1977; Mikawa et al., 1996). Microscopic analysis of the phage capsid identified easily accessible and protruding domains of the trimer protein gpD (Sternberg and Hoess, 1995). It was also discovered that gene *D* deficiency can be complemented by the expression of *D in trans* (Sternberg and Weisberg, 1977). These findings led to wide exploitation of *D::X* translational fusions as a tool to express proteins and peptides of interest on the surface of the phage λ capsid (Mikawa et al., 1996). The proteins fused to the capsid D protein can be expressed without interfering with the capsid assembly of the phage, thus producing phage capsids that display functional recombinant proteins (Mikawa et al., 1996) (Figure 5). Gupta et al., (2003) described a successful phage λ display system that displayed various peptides and full length proteins fused to the C-terminal end of the D capsid protein and found that phage λ had a maximum of 420 fused particles per phage capsid, which was significantly higher than the widely used M13 phage that can only incorporate a handful of fusions (Casjens & Hendrix, 1974; Gupta et al., 2003).

The application of phage display in biotechnology has grown remarkably over the years to generate protein expression libraries, nanowires for microcircuitry applications, sensors for food and water borne pathogens in outbreaks and bioterrorism attacks, insecticides and antibacterial therapeutics to just name a few (Vilchez et al., 2004; Petty et al., 2007; Bratkovic, 2009). However, despite

a plethora of applications, the ability to control the expression of the fusion has until very recently, remained crude at best, while essential toward the best functionality of a construct. Hayes et al., (2010) demonstrated a system whereby fusion was controlled by plasmid carrying fusion inserts under the regulation of a temperature-sensitive repressor, and applied this approach to the expression of porcine Circovirus 2 peptides that elicited immunogenic reaction in pigs. More recently, Nicastro et al. (2013) demonstrated a highly tuneable phage display system. Using a *D::eGFP* fusion, we employed the λ *cI*[Ts]*857* temperature-sensitive repressor to regulate expression of *D::eGFP* fusions. Temperature sensitive repressor λ*cI*[Ts]*857* –mediated production of the gpD::eGFP fusion was combined with a second level of control using amber suppressor allele-mediated suppression. The passaged λ *Dam15* phage generated a wide variety of decoration permutations of D::eGFP protein fusions displayed on the λ capsid, by changing the temperature and the suppressor genetic background of the host. The ability to control decoration can be essential to mitigate negative decoration or incorporation effects generated by steric hindrance of protruding fusions, or to control avidity in important ligand interactions.

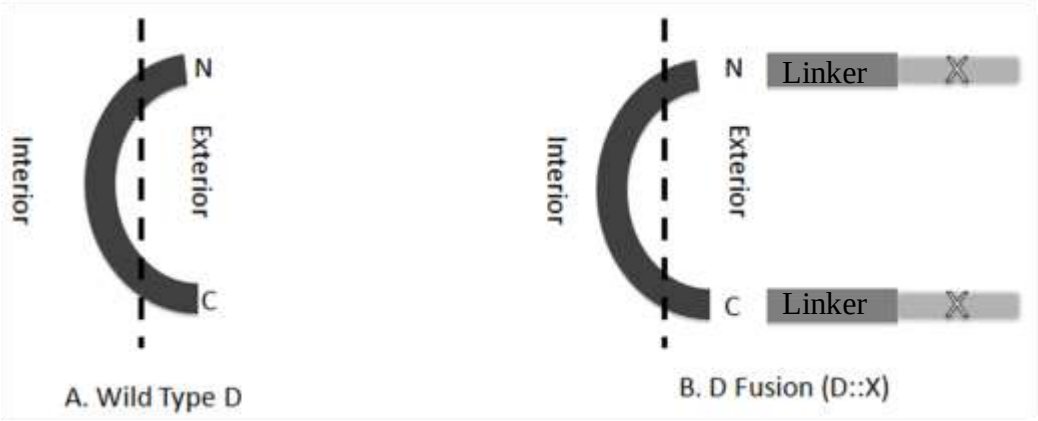

Figure 5. Schematic of λ wild type major capsid protein D(A) and D fusion (gpD::X) (B). Endolysin and it domains fusions linked to the N and C-termini of protein D (as depicted by X, in Figure 5B). Linker length is 10 amino acids.

Dimension 1: CI[Ts]857 repressor regulation of D::X fusion expression

The first dimension of decorative control in the phage λ display system was imparted by the λ temperature sensitive repressor CI857, encoded on the pPL451 plasmid below (Figure 6; Love et al., 1996). Gene expression in pPL451 is turned off at low temperatures where the CI857 repressor is fully active and thus fully capable of blocking expression from the strong λ *pL* and *pR* promoters that drive expression of downstream gene(s) of interest. Upon shifting temperature to ~ 37° C or higher, CI857 is inactivated and can no longer prevent expression from *pR* and *pL* promoters, and gene expression ensues (Love et al., 1996; Valdez-Cruz et al., 2010).

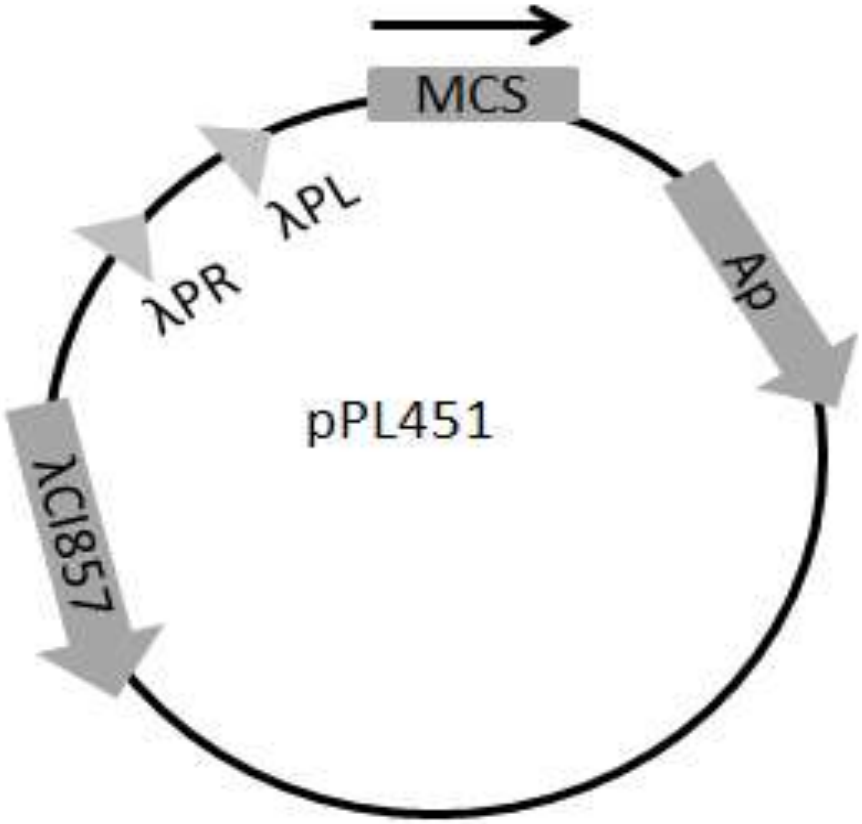

Figure 6. pPL451 map. pPL451 is a cloning vector. pPL451 carries the Ap selection marker. Cloned genes are inserted in MCS. Expression of genes in MCS is regulated by λ promoters (*pR*- right promoter and *pL*- left promoter).

Dimension 2: Amber stop codon suppressor alleles

A nonsense mutation, mutation from encoding a glutamine to an amber stop codon (TAG) was located in *Dam15* allele of the λ*imm21Dam15* phage that serves as the infecting phage for tuneable decoration. *The Dam15* mutation forms a stop codon at the 68th residue of the *Dam15* allele that results in a truncated gpD derivative when expressed in a wild type (nonsuppressor; Sup-) strain. When λ*imm21Dam15* infects a Sup- strain it is incapable of producing a functional gpD due to the early termination of translation of protein D and as

such, the phage cannot properly assemble and is unviable (Herskowitz, 1973; Nicastro et al., 2013). In contrast to its unsuccessful growth on Sup- cells, λ*imm21Dam15* phage is able to grow on suppressor positive (Sup^+) mutant strains of *Escherichia coli* (*E. coli)* (notably SupD and SupE) that contain tRNAs that read through the stop codon and instead of terminating translation, insert a particular amino acid instead, thereby producing full length gpD alleles with varying functionality compared to the wild type pristine sequence (Table 1). SupE inserts a glutamine at the 68^{th} position of Dam15 upon its translation, restoring its pristine sequence, while SupD inserts a serine at this site and severely compromises the allele's functionality (Herskowitz, 1973; Nicastro et al., 2013).

Table 1. Suppressor Negative and Positive strains.

	Cell Strain		
	Sup-	**SupD**	**SupE**
Genotype	Amber stop codon	Serine substitution	Glutamine substitution
Phenotype	Truncated gpD	Serine substitution	Glutamine substitution
Protein Produced	Truncated (68 a.a)	Full (110 a.a)	Full (110 a.a)

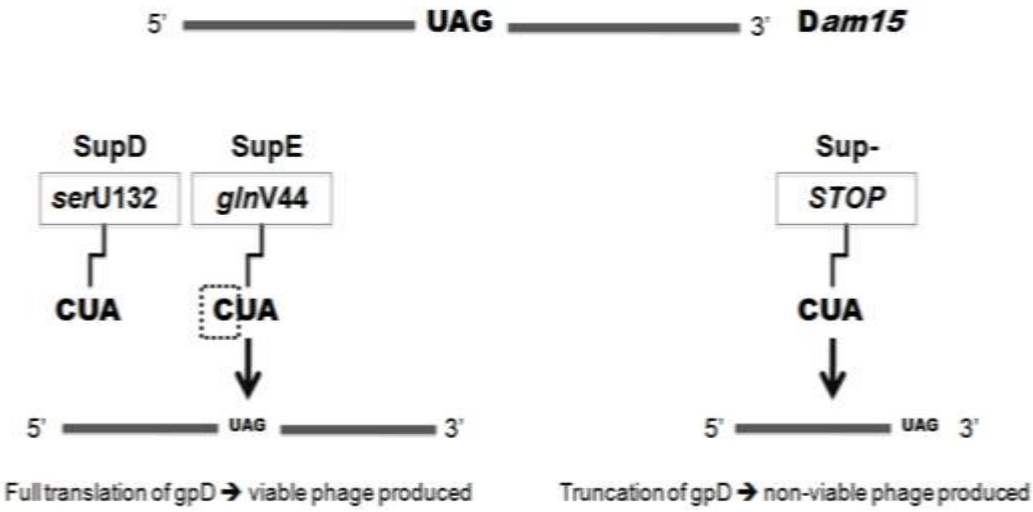

Figure 7. *Dam15* Amber stop codon non-suppression and suppression in different host strains.

In this study, we used phage λ*imm21Dam15* capsid as a scaffold to display endolysin K and its domains derivatives as fusions to the λ major capsid protein, gpD employing the genetic control of the two genetic elements described above. The decorated phage with endolysin K and its domains were assayed for their ability to serve as lytic nanoparticles when added to susceptible *S. aureus* strains under a variety of conditions. The display of active functional proteins on phage λ capsids holds several advantages over the large—scale production of recombinant proteins. This is particularly evident with respect to the reduced cost of production compared to recombinant proteins, since cloning and passaging of phage on host strains is much simpler and offers superior efficiency (Beghetto & Gargano, 2011). In addition, phage can remain stable at both room temperature and at 4° C when supplied with divalent cations, glycerol and neutral pH for long term stability (Filatova et al., 2010; Beghetto & Gargano, 2011) and as such offer great potential as therapeutics in less developed countries.

It is worth to mention that the phage λ that will be used in this study to display gpD::LysK and its domains fusions is only used as a scaffold to present LysK and its domains to the clinically relevant *S. aureus* strains. Phage λ will not be able to infect *S. aureus* strains due to specificity constraints (tail proteins on phage λ can not recognize attachment sites on *S. aureus* peptidoglycan) (Fig. 8).

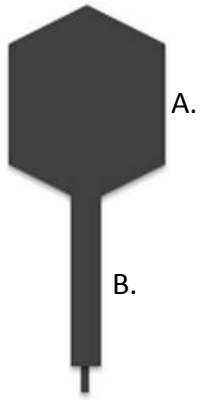

Figure 8 Schematic of λ Phage

A. Phage λ capsid B. Phage λ tail

Chapter 2: Rationale, Objectives and Hypothesis

Rationale

The process of displaying foreign proteins on phage is a much more rapid process than expressing and purifying soluble proteins from bacterial expression hosts. Insoluble proteins that were produced as inclusion bodies in the cytoplasm of host cells were soluble when displayed on phage. The display of foreign fusion proteins to major capsid protein D enables the display of 405-420 fusions which is much higher display efficiency compared to other display systems. In general, the display of fusion proteins is a cost efficient procedure since it doesn't require sophisticated instrumentation or material. Phage can be freeze dried when trehalose or sucrose were added to them, also the transportation of phage lysates is feasible since phage preparations can remain stable for 5-6 months at room temperature. The successful display of functionally lytic LysK and its domains for targeting *S. aureus* strains will open the doors for displaying other lysins that are specific for the lysis of other gram positive strains, hence developing phage cocktails that display various lysins targeting various gram-positive species. The unavailability of new classes of antibiotics to fight antibiotic resistant strains, the side effects and side reactions that are associated with antibiotic use and toxicity of antibiotics mandate the need to develop new unexploited and effective antibacterials.

Objectives

The objectives of this work are outlined below:

- To design and construct a system for phage λ particle-based display of endolysin K and its various domains on the surface of phage λ. This objective involves the fusion of LysK domains to the gpD capsid protein via exploitation of either amino or carboxy terminal fusions.
- To characterize the phage display constructs created for resultant phage viability and hence, functionality of gpD fusions. This objective includes assessing the ability of *D::X* fusions to complement the *Dam15* mutation and to assess the optimal conditions for complementation and decoration.
- To assess the lytic capabilities of phage display products on various strains of *S. aureus.* This objective involves the qualitative and quantitative assessment of gpD::X protein fusions and decorated phage as lytic antimicrobial agents of MRSA, VRSA and bovine *S. aureus.*
- To purify and characterize gpD::X endolysin proteins and assay their activity when not integrated in the phage capsid.

Hypothesis

The fusion of lytic and specificity domains of LysK to amino- and/or carboxy-terminal ends of the gpD capsid protein will produce functionally lytic particles against clinically relevant *S. aureus* strains.

Chapter 3: Materials and Methods

Growth media

Luria Bertani (LB) broth (Becton Dickinson, Mississauga, Canada): Rich broth for growth of bacterial cultures. Tryptone 10 g, yeast extract 5 g and NaCl 10 g per L of ddH_2O. Broth was then autoclaved for 30 min to sterilize and antibiotics were added as necessary to cooling medium. Antibiotic concentrations: ampicillin (Ap) 100 μg/mL; kanamycin (Kn) 50 μg/mL and chloramphenicol (Cm) 20 μg/mL. Antiobiotics were added from concentrated stock solutions, Ap in H_2O; Kn in H_2O; Cm in ethanol. Stock antibiotic solutions of Ap and Kn were stored at -20^{o} C.

Luria Bertani (LB) agar (Becton Dickinson, Mississauga, Canada): Main solid media that was used to plate bacterial cultures. Tryptone 10 g, yeast extract 5 g, Sodium Chloride 10 g and agar 15 g per L of ddH_2O. After autoclaving for 45 min to sterilize, plates were prepared by pouring approximately 35 mL of cooling agar into sterile Petri plates (Fisher Brand, Ottawa, Canada). Antibiotics were added as necessary: Ap, 100 μg/mL, Kn, 50 μg/mL, Cm, 20 μg/mL to cooling media before pouring then plates were left overnight at room temperature (RT).

Brain Heart Infusion (BHI) broth (Becton Dickinson, Mississauga, Canada): Very rich liquid broth growth medium used to culture *S. aureus*. BHI from solids 3.5 g, peptic digest of animal tissue 15 g, pancreatic digest of casein 10 g,

dextrose 2 g, NaCl 5 g and disodium phosphate 2.5 g per 1 L of ddH_2O. Media was autoclaved for 30 min to sterilize then stored at 37 °C.

Brain Heart Infusion (BHI) agar (Becton Dickson, Mississauga, Canada): Main solid media that was specifically used to plate *S. aureus* cultures. Brain Heart infusion from solids 8 g, Peptic digest of animal tissue 5 g, Pancreatic digest of Casein 10 g, Dextrose 2.5g, Sodium Chloride 5 g, Disodium Phosphate 2.5 g and agar 13.5 per 1 L of ddH_2O. After autoclaving for 45 min to sterilize, plates were prepared by pouring approximately 35 mL of cooling agar into sterile Petri plates (Fisher Brand, Ottawa, Canada). Antibiotics were added as necessary, Ap 100 μg/mL, Kn 50 μg/mL, Cm 20 μg/mL to cooling media before pouring then plates were left overnight at RT.

Top Agar: Used to resuspend phage and cells on top of solidified media plates. Tryptone 10 g, yeast extract 5 g, Sodium Chloride 5 g and agar 7 g per 1 L of ddH_2O. After proper mixing, media was poured into bottles to be sterilized by autoclaving for 30 min. Media was stored in sterile media bottles at 50° C.

Super Optimal Broth (SOC): Used as recovery media for electroporated cells. Preparation is similar to LB broth media with the addition of tryptone 10 g, $MgCl_2$ 1 M and glucose 1M. Media was autoclaved for 30 min to sterilize, then stored at 37° C.

Buffers

TN buffer: Tris NaCl buffer used to provide a suitable pH to dilute and passage phage. Tris base (Fisher Bioreagents, Ottawa, Canada) 0.01 M, Sodium Chloride (Fisher Bioreagents, Ottawa, Canada) 0.1 M, pH adjusted to 7.8 with HCl (Fisher Brand, Ottawa, Canada). Buffer was autoclaved for 30 min to sterilize and stored at RT.

TN (TN + EDTA) buffer: Used to conduct phage EDTA sensitivity assays as mutant phage capsids have been shown to be unstable in presence of EDTA. Tris base 0.01 M, Sodium Chloride 0.1M, 10.0 mM EDTA (Fisher Bioreagents, Ottawa, Canada) pH adjusted to 7.8 with HCl. Buffer was autoclaved for 30 min to sterilize and stored at RT.

1X TAE Buffer: Used as buffer that provides ions and suitable pH to separate DNA fragments by size by gel electrophoresis**.** 50X TAE (Fisher Bioreagents, Ottawa, Canada) was diluted in ddH_2O for a total volume of 30 L and stored at RT.

10% Laemmli Running Buffer: Used as buffer that provides ions and suitable pH to separate protein by size by SDS-PAGE. Tris base 30 g, Glycine (EMD, Frankfurter, Germany) 144 g, SDS 10 g per 1 L of ddH_2O**.** A 1X dilution of Laemmli running buffer was prepared prior to running the gel.

Laemmli Loading Dye Buffer (Bio-Rad, Mississauga, Canada): Used as loading buffer to visualize protein samples running in SDS-PAGE gel. 50 µL of β-mercaptoethanol was added to 950 µL of Laemmli sample buffer (Bio-Rad,

Mississauga, Canada) to a final concentration of 710 mM. Loading buffer was added at a 1:1 ratio of buffer to protein.

Dialysis Buffer: Used as an exchange buffer to dialyze proteins in elution buffer. 20 mM Tris base, 20 mM NaCl, 5 mM $CaCl_2$ (Fisher Brand, Ottawa, Canada) and 50% glycerol (EMD, Frankfurter, Germany). 20 mL of 1 M Tris base, 20 mL of 1 M NaCl, 5 mL of $CaCl_2$ and 500 mL of glycerol were mixed in 1 L of ddH_2O. Buffer was autoclaved for 30 min to sterilize and stored at RT.

Additional solutions and reagents:

Polyethylene Glycol (PEG) 8000 (Fisher Brand, Ottawa, Canada)**:** Used to precipitate phage lysates by binding to them. 20 g PEG and 14.6 g NaCl were dissolved in 100 mL of ddH_2O. After mixing, the solution was filter sterilized with AcroVac Filter Unit, 0.2 μm PES membrane (VWR International, Mississauga, Canada).

Isopropyl β-D-1-thiogalactopyranoside (IPTG; Fisher Bioreagents, Ottawa, Canada): Used to induce protein expression in pET30a+ expression vector. IPTG powder 2.38 g (Sigma, Oakville, Canada) was dissolved in 100 mL of ddH_2O to make a 100 mM IPTG solution. The solution was filter sterilized and stored at -20° C.

Sodium Dodecyl sulfate (SDS; Bio-rad, Mississauga, Canada): Used to denature and unfold proteins, providing a negative charge to polypeptides. 20% SDS was used to denature and apply same charge per unit length to proteins

analyzed by electrophoresis. 10 g SDS was dissolved in 40 mL of ddH_2O and aliquots of 1 mL were stored at -20° C.

10% Ammonium persulfate (APS; Bio-Rad, Mississauga, Canada): Used to generate free radicals and catalyze the gel polymerization reaction. 1 g was dissolved in 10 mL of ddH_2O. Aliquots of 100 mL were stored at -20° C.

Antibiotic Preparations

Ampicillin (Ap): Stock solution was prepared at a concentration of 100 mg/mL by dissolving ampicillin trihydrate powder (MP Biomedicals, Montreal, Quebec, Canada) into ddH_2O and storing at -20° C.

Kanamycin (Kn): Stock solution was prepared at a concentration of 50 mg/mL by dissolving kanamycin monosulfate powder (MP Biomedicals, Montreal, Quebec, Canada) into ddH_2O and storing at -20° C.

Chloramphenicol (Cm): Stock solution was prepared at a concentration of 20 mg/mL by dissolving chloramphenicol powder (MP Biomedicals, Montreal, Quebec, Canada) into 95% ethanol and storing at -20° C.

Gel Preparations

0.8% DNA Agarose Gel: Used to run and visualize DNA samples. Agarose gel was prepared by dissolving 0.8 g of ultrapure agarose (Fisher Bioreagents, Ottawa, Canada) into 100 mL of 1X TAE buffer. The agarose was dissolved by microwaving the solution for 45-60 s. 5 µL of ethidium bromide (EtBr; Bio-rad,

Mississauga, Canada) was added to the cooling agar prior to pouring into the gel cast.

SDS-Polyacrylamide Gel (SDS-PAGE): Used to run and visualize protein samples. The SDS gel is comprised of 2 parts: the resolving and the stacking gel.

Reagent	**Resolving gel 12.5%**	**Stacking Gel 6%**
30:0.8% w/v acrylamide:bisacrylamide (Bio-Rad, Mississauga, Canada)	3.1 mL	1 mL
1.0M Tris_HCl pH 8.8	3 mL	630 µL
20% SDS	38 µL	25 µL
dH_2O	1.3 mL	3.6 mL
10% APS	36 µL	25 µL
TEMED	5 µL	5 µL

Strains and Plasmids: Strains of bacteria, phage and plasmids used in this research are shown and described in Table 2.

Table 2. Bacteria, Phage and Plasmids

Designation	Relevant Properties	Source
Phage		
λF7	λ*imm21Dam15cIts*	Lederberg (1951)
λF7-D::LysK	λF7 expressing LysK on capsid surface	This study
λF7-D::CHAP	λF7 expressing CHAP on capsid surface as C-terminal gpD fusion	This study
λF7-CHAP::D	λF7 expressing CHAP on capsid surface as N-terminal gpD fusion	This study
λF7-D::SH3	λF7 expressing SH3 on capsid surface	This study
λF7-CHAP::D::SH3	λF7 expressing CHAP and SH3 on capsid surface	This study
λF7-D::Bind	λF7 expressing Bind on capsid surface	This study
Bacterial Strains		
BB4	*supF58 supE44 HsdR514 galK2galT22 trpR55 metB1 tonADE(lac)U169*	Agilent Technologies, Inc.
W3101	F-, *galT22*, λ-, IN*(rrnD-rrnE)1, rph-1*	CGSC #4467, Bachmann (1972)
W3101 *supD*	F-, *galT22*, λ-, IN*(rrnD-rrnE)1, rph-1, uvrC279::Tn10, serU132(AS),*	Nicastro et al. (2013)

W3101 *supE*	F-, *galT22*, λ-, IN*(rrnD-rrnE)1, rph-1, crcA280::Tn10, glnV44(AS),*	Nicastro et al. (2013)
JM109	*endA1 glnV44 thi-1 relA1 gyrA96 recA1 mcrB*$^{+}$ *Δ(lac-proAB) e14- [*F' *traD36 proAB*$^{+}$ *lacI*^{q} *lacZ*ΔM15] *hsdR17(*$r_K^- m_K^+$*)*	New England Biolabs # E4107S, Whitby, Canada
DH5α	F-, *Δ(argF-lac)169, ϕ80dlacZ58(*M15*), ΔphoA8, glnV44(*AS*)*, λ-, *deoR481, rfbC1, gyrA96 (NalR), recA1, endA1, thi-1, hsdR17*	CGSC #12384
Rosetta	F$^-$ *ompT hsdS*$_B$ *(*$r_B^- m_B$*) gal dcm lacY1pR*ARE6 (Cm^R)	
Mu50	hVRSA, heterogeneous vancomycin resistant *Staphylococcus aureus*	ATCC #700699, Manassas, Virginia, USA
DPC5246	bovine *Staphylococcus aureus*	Gift from Teagasc Food Research Centre, Ireland
DPC5645	MRSA, methicillin resistant *Staphylococcus aureus*	Gift from Teagasc Food Research Centre, Ireland
Plasmids		
pPL451	*PL-cI857-tm*	Love et al. (1996)
pKS2 (pPL451 gpD)	*PL-cI857-D*	Nicastro et al. (2013)
pKS1(pPL451 gpD::eGFP)	*PL-cI857-D::eGFP*	Nicastro et al. (2013)
pEF-1 (pPL451 *D::lysk*)	*pM-cI857-pL-cI857-pL-D::lysk-tL*	This study
pEF-2 (pPL451	*pM-cI857-pL-cI857-pL-*	This study

D::CHAP)	*D::CHAP-tL*	
pEF-3 (pPL451 *CHAP::D*)	*pM-cI857-pL-cI857-pL-CHAP::D-tL*	This study
pEF-4 (pPL451 *D::bind*)	*pM-cI857-pL-cI857-pL-D::Bind-tL*	This study
pEF-5 (pPL451 *D::SH3*)	*pM-cI857-pL-cI857-pL-D::SH3-tL*	This study
pEF-6 (pPL451 CHAP::D::SH3)	*pM-cI857-pL-cI857-pL-CHAP::D::SH3-tL*	This study
pOG-1 (pET30a+ *D::lysk*)	*pT7-His::D::lysk*	This study
pOG-2 (pET30a+ *D::CHAP*)	*pT7-His::D::CHAP*	This study
pOG-3 (pET30a+ *CHAP::D*)	*pT7-His::CHAP::D*	This study
pOG-4 (pET30a+ *D::Bind*)	*pT7-His::D::Bind*	This study
pOG-5 (pET30a+ *D::SH3*)	*pT7-His::D::SH3*	This study
pOG-6 (pET30a+ CHAP::D::SH3)	*pT7-His::CHAP::D::SH3*	This study

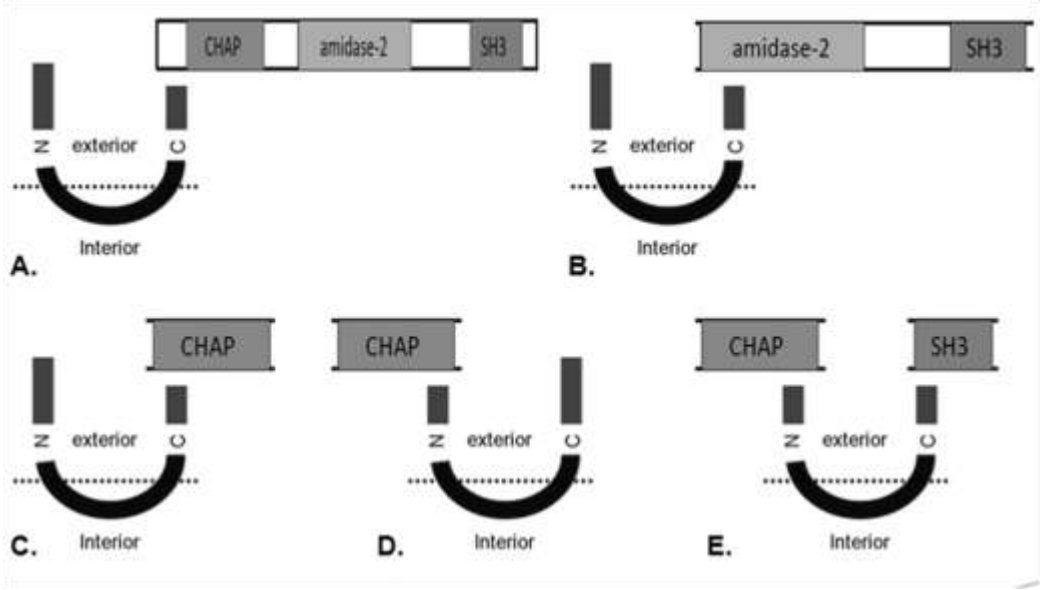

Figure 9. Different constructs of LysK and its domains fused to gpD. A. full length LysK lysine fused to C terminus of gpD B. Amidase-2 catalytic domain and SH3 specificity domain fused to C terminus of gpD C. CHAP catalytic domain fused to C terminus of gpD D. CHAP catalytic domain fused to N terminus of gpD E. CHAP catalytic domain fused to N terminus of gpD while SH3 specificity domain fused to C terminus of gpD.

Methods

Construction of pPL451 plasmids: *D::lysk* and its derivatives were synthesized (GenScript Inc., New Jersey, USA) and cloned into pPL451 at the *Bam*HI and *Hind*III restriction enzyme sites of the multiple cloning site (MCS).

Preparation of Electrocompetent *E. coli* cells: Electrocompetent cells need to be grown to certain number of cells and washed several times with ice cold water to remove all charged particles that could interfere with the electroporator's electric pulse. A 1:100 dilution of fresh ON culture at OD_{600} = ~2.0 was prepared and incubated at 37° C with shaking at 200 RPM for 3-4 h, or until OD_{600} = 0.4-0.5. The culture was then incubated on ice for 10 min before spinning down cells at 4K RPM for 10 min at 4° C. Cells were resuspended in 20 mL of ice chilled sterile ddH_2O, spun down and resuspended in half volume (10 mL) ddH_2O, before being spun down and resuspended in a final volume of 0.5-1.0 mL. Cells were then either electroporated immediately, or stored for future electroporation in 10% glycerol at -80° C.

Electroporation: Electric pulse opens pores in the cell membrane that will enable plasmid to enter the cells. A plasmid solution of 500-700 ng was added to 50-90 µL of electrocompetent cells and incubated on ice for 10 min. The mixture was then added to electroporation cuvettes and pulsed at 1000 V in an Electroporator 2510 (Eppendorf, Mississauga, Canada). Electroporated cells were immediately resuspended in 1 mL of fresh SOC media and incubated for 1 h at 37° C, 50 RPM. Cells were then centrifuged at 13K g for 5 min; the pellet

was then resuspended in 200 µL of SOC media and plated on selection plates with antibiotics. Plates were then incubated overnight at 37° C.

Plate Lysate Preparation and Purification: Cells harbouring plasmids were grown overnight at 30° C, 200 RPM. A 1:100 dilution was prepared from the overnight culture and cells were grown at 30° C to OD_{600} 0.4-0.5. Cells were then induced for 2 h at 37° C-40° C before plating with 10^{-1} -10^{-3} PFU/mL λF7 lysate and 3 mL of Top agar on LB + Ap plates. A 10^4 fold dilution of a 1 X 10^{10} PFU/mL lysate of λF7 lysate was added to 300 µL of fresh overnight culture of BB4 cells, 3 mL of Top agar and plated on LB plates. Plates were incubated over night at 37˚ C. To plates showing adequate semi-complete lysis pattern, 10 mL of sterile TN buffer was added and incubated for 4-24 h at 4˚ C. Top agar was scraped and the buffer was collected into conical tubes with 50 µL of chloroform added. Lysates were incubated on ice for 10 min. Lysates were centrifuged at 14K RPM for 40 min (Avanti J-E Beckman Coulter, Mississauga, Canada) to remove the Top agar and cellular debris. Lysate was further purified by passaging through 0.45 µm polyethersulfone filter membrane (VWR, Mississauga, Canada) then stored at 4° C.

Precipitation of Lysates: PEG binds to phage particles and precipitates them while centrifuging. PEG stock solution was added to phage lysate at 1:4 ratio. The mixture was then incubated on ice for 30 min before centrifuging for 40 min at 11K RPM at 4^o C. The supernatant was poured out and the pellet was spun again 2-3X to completely dry it. The phage pellet was then resuspended in 1 mL of TN buffer and stored at 4° C.

Plate Overlay Lysate Titration: This assay was performed to quantify phage, by way of plaque forming units, in the freshly prepared lysates. Phage lysates were plated on double suppressor strain BB4 as a 100% plating control. Each plaque grown corresponds to one phage particle allowing for phage to be quantified relative to the ideal BB4 host for propagation. All serial dilutions of prepared lysates were prepared in TN buffer. 300 µL of fresh overnight culture of BB4 and 3 mL of top agar were plated on LB plates. Next, 10 uL of each lysate dilution was added to the solidified top agar overlay. Plates were then incubated overnight at 37˚ C and plaques were counted.

Assessing ability of gpD::endolysin fusions to complement gpD deficiency in λF7 capsid assembly: A complementation assay was employed to assess how efficiently gpD::X fusions could complement for the gpD genetic deficiency of λF7, thereby enabling phage DNA compaction and capsid assembly. A 1:100 dilution of fresh overnight culture of W3101 Sup- [pPL451_insert] and SupD [pPL451_insert] were prepared and grown at 30° C, 200 RPM for 3-4 h or to A_{600}=0.4-0.6. Next, 300 uL of each culture was incubated for 2 h with no shaking at induction temperatures 30˚ , 35˚, 37˚, and 39-40˚ C. Aliquots were next plated on LB + Ap plates with 3 mL of top agar overlay. Serial dilutions of λF7 were prepared in TN buffer. The λF7 dilutions were then plated on the solidified Top agar and then incubated overnight at the induction temperatures.

Phage Lysis Assays: This assay was performed to assay the ability of displayed phage to elicit lytic activity against bovine *S. aureus* strains. A 30 µL aliquot of fresh overnight culture of bovine *S. aureus* was plated on brain heart infusion

plates with 3 mL of Top agar. Standardized displayed lysates of 10^6 - 10^7 PFU/mL were added to the plate overlay. Next, 10 µL of TN buffer and $CHCl_3$ (chloroform) were added to plates as negative and positive controls, respectively. Plates were then incubated overnight at 37° C.

EDTA Phage Sensitivity Assays: This assay was performed to test the stability of the displayed proteins on the phage capsid. Lysates from Sup- W3101 and the SupD derivative were standardized to 10^7 - 10^8 PFU/mL. One set of lysates was treated in TN buffer + EDTA for 21 min at room temperature, and then diluted to 10^{-6}-10^{-7}/10^{-7}-10^{-8}. Lysates were then mixed with 300 µL of fresh overnight culture of BB4 indicator cells and incubated at 37° C on LB plates. Lysates treated only with TN buffer served as control. These dilutions were also plated with BB4 indicator cells on LB plates. All plates were then incubated overnight at 37° C.

Plasmid Extraction: This common procedure that is known as miniprep was performed for small scale isolation of plasmids from cells. Plasmid pPL451 constructs growing in 10 mL of fresh overnight culture grown at 37˚ C, 200 RPM in LB + Ap were extracted using a Plasmid Mini Kit I (Omega Bio-Tek, Norcross, USA) according to supplier instructions. The kit is based on alkaline precipitation of episomal DNA. Plasmid DNA was eluted with 80-100 µL of DNase/RNase free molecular grade water (Hyclone, Ottawa, Canada). DNA concentration was determined using a Nanodrop 2000 spectrophotometer at A_{260} (Thermo Fisher Scientific, Ottawa, Canada).

Plasmid Digests: This assay was conducted to digest and move out DNA segments from plasmids for subsequent cloning experiments. Digestion reactions were set up using 1 μg of pPL451 or pET30a+ plasmid DNA, 10 IU of each of BamHI HF and HindIII HF restriction enzymes (New England Biolabs Whitby, Canada), 1X NEB buffer 4 and DNase/RNase free molecular grade water (Hyclone, Ottawa, Canada). A negative control digest reaction was run with constructs without inserts. All digest samples were incubated in 37° C water bath for 1-3 h.

Purification of DNA fragments: Gel Electrophoresis was used to visualize EtBr-DNA complexes. DNA fragments from DNA digests were run against a 1 Kb DNA ladder (New England Biolabs, Whitby, Canada) on a 0.8% agarose gel with 2 μL EtBr (Fisher Bioreagents, Ottawa, Canada) at 100 V for 1 h. Gel was then observed under Spectroline UV Transilluminator (Thermo Fisher Scientific, Ottawa, Canada). DNA fragments possessing genes of interest were identified based on their correct size. Individual bands were cut from the gel and purified using Omega Gel Extraction Kit (Omega-Bio-Tek, Norcross, USA). Protocol was followed exactly as supplied. Inserts were eluted with 30-50 μL of DNase/RNase free molecular grade water. Concentration of inserts was determined using a Nanodrop 2000 spectrophotometer (Thermo Fisher Scientific, Ottawa, Canada). In contrast to insert DNA preparation, digested vector pET30a+ DNA was purified using a PCR Cycle Pure Kit (Omega Bio-Tek, Norcross, USA) as per supplier instructions.

DNA cloning: This procedure was used to construct new customized plasmids carrying the genes of interest for expression. Ligase enzyme forms a bond between terminal ends of each of the insert and plasmid. Ligation reactions were set up with 200 ng of vector and insert was added in a minimal volume at a 1:3 ratio, along with 1X of ligase buffer, 1.5 μL of T4 DNA ligase (New England Biolabs, Whitby, Canada) and DNase/RNase free molecular grade water. In all cases, a negative control reaction was carried out without added insert. Ligation reactions were incubated overnight at 16 - 25° C.

Cell transformation, selection and clone screening: Electrocompetent cells were prepared as described above. A 10 μL of ligation reaction was added to 90 μL of electrocompetent cells. The ligation- cell mixture was then added into electroporation cuvettes and mixture was electroporated at 1000 V. A 1 mL of SOC broth was added to electroporated mixture and incubated at 37° C, 50 RPM for 1-1.5 h. To collect all cells, ligation-cell mixture was then centrifuged at 10K g for 5 min to pellet the cells. Cell pellet was then resuspended in 200 μL of LB broth, plated on LB + Kn plates and incubated at 37 °C ON. Random single colonies were picked up from overnight grown plates and cultured overnight in LB + Kn broth at 37° C, 200 RPM. The plasmids were then extracted using Plasmid Mini Kit and concentrations were determined. Next, 500-700 ng of extracted plasmid was digested with HindIII_HF and BamHI_HF for experimental plasmids and with HindIII_HF and KpnI for LysK positive control plasmid construct. Digests were then run on a 0.8% agarose gel (described

earlier). Plasmids carrying the fragment of interest were identified by restriction digest pattern analysis.

Insert DNA sequencing: A 200-300 ng sample of selected clones demonstrating proper digestion patterning were prepared in 7 µL of DNase/RNase free molecular grade water and submitted to TCAG sequencing facility (The Center for Applied Genomics, Toronto, Canada).

Assessment of Protein Expression: Rosetta cells harbouring constructed pET30a+ plasmids and Rosetta strains with pET30a+ only and with no plasmid were grown overnight shaking at 37° C, 200 RPM in LB + Kn broth. The next day, 1:100 dilutions were made from fresh overnight cultures and were grown at 37° C, 200 RPM for 6-8 h or until OD_{600}= 0.8. Cells were then induced with 1 mM IPTG and grown for 1-2 h or until OD_{600}= 1-1.2. Cells were then centrifuged at 4K RPM for 10 min, washed three times with ice cold sterile water and then the pellet was stored at -80° C. A mechanical cell disruption procedure was performed to extract the expressed proteins from the cells. Rosetta cell pellets harbouring constructed pET30a+ plasmids were resuspended in 1 mL of ice cold sterile water. Cells were then sonicated (mechanical cell disruption) three times for 45 s at setting frequency of 4.5, in 2 min intervals. Next, lysates were centrifuged at 13K PM at 4° C for 10 min. Protein crude extracts were stored at -20° C.

BCA Pierce Protein Assay: This assay was conducted to determine the concentration of the extracted proteins. The protein concentration of the crude extracts was assayed by a Pierce BCA Protein Assay Kit (Thermo Fisher Scientific, Ottawa, Canada) according to the manufacturer's instructions and samples were interpolated against a BSA standard protein curve from 500-1250 μg/μL.

His60 Nickel (Ni) Gravity Column Extraction: LysK and its domain constructs were purified from the cell's background proteins by passing the protein crude lysates through Ni columns. His tagged proteins from crude lysates were purified using a His60 Ni Gravity Column Purification Kit (Clontech, Mountain View, USA) according to manufacturer's instructions.

Zymogram Lysis Assay with Standardized proteins: This assay is performed to test the lysis activity of the extracted proteins. A 30 μL sample of fresh culture of bovine *S. aureus* was plated with 3 mL of Top agar on BHI plates. A 100 μg aliquot of protein crude lysates was then added to the solidified Top agar before incubating plates overnight at 37° C. Plates were examined the next day for lysis by observing a clearing zone where the protein lysate was added. Buffer used for protein lysates incubation was used a negative control.

SDS Gels of Column Purified Samples: A 200 μg sample of purified protein was run for 20 min at 60 V, then for 2-2.5 h at 100 V, separating proteins by SDS-PAGE. EZ run Rec protein ladder (Thermo Fisher Scientific, Ottawa, Canada) was run along the samples for size determination of separated proteins.

Gels were then incubated for 5 min in 25% isopropanol and 8% acetic acid to fix proteins. Gels were then washed 3 times in ddH_2O water and stained overnight with gel code staining solution (Thermo Fisher Scientific, Ottawa, Canada).

Protein Dialysis: This procedure was performed to exchange the buffer in protein samples with buffer containing cofactors that enhance the activity of LysK catalytic domains. Protein samples were placed in a device that possesses a cellulose membrane. The device was then placed in a conical tube filled with 1.75 mL-45 mL dialysis buffer. The conical tube was incubated for 6 h at 4° C with one time exchange of dialysis buffer at 3 h.

Inhibitory Concentration Assays: These assays was performed to check the inhibitory concentrations of LysK and its derivatives antibacterial constructs required to kill a standardized number of bovine *S. aureus* strains. Protein crude lysates were standardized to 7.5 µg, 15 µg, and 37.5 µg. A 1:100 dilution of fresh overnight culture of bovine *S. aureus* was prepared and incubated at 37° C and 200 RPM for 1-2 h or until OD_{575} = 0.1. 1:10 and 1:100 serial dilutions of the bacterial culture of 10^8 CFU were prepared in ultrapure ddH_2O and added to each of the 5 concentrations of protein crude lysates and incubated at 37 °C for 1 h. After incubation, 3 mL of Top agar was added to the protein- cell mixture and then plated on BHI plates and incubated ON at 37° C. Negative control samples or untreated samples were cells added to ultrapure ddH_2O and plated. CFU counts were scored the following day and surviving cells was divided by untreated cells to determine the efficiency of plating.

Chapter 4: Results

Complementation of λ Dam15 and gpDQ68S alleles by gpD::X endolysin-capsid fusions.

We exploited the packaging requirements of phage λ to determine the ability of our fusions to be incorporated and stabilize the capsid to generate viable phage progeny. The phage λ*imm21Dam15* mutant encodes a truncated and inactive form of the gpD protein necessary for packaging of the full length 48.5 kb phage genome. In the *E. coli* nonsuppressor W3101 strain (Sup-), gpD is not formed and the phage λ*Dam15* mutant is incapable of plaque formation (growth). As such, inducible *D::lysk* derivatives can be assessed in this strain for their ability to complement the *Dam15* deficiency *in trans* compared to growth of the phage on a suppressor strain, BB4 (*supE supF*), that suppresses the *Dam15* mutation and imparts translation of the pristine gpD_{wt} sequence. The ability of *D* expressed from plasmid pPL451 to complement the *Dam15* deficiency of the infecting phage increased, as the inducing temperature increased. The CI857 repressor is temperature-labile and loses activity exponentially at temperatures above 37^{o} C. Therefore, at 30^{o} C the repressor efficiently blocks expression of the *D::eGFP* fusion preventing complementation of the *Dam15* mutation. However, as the temperature is raised and CI857 loses activity, expression increases, resulting in improved complementation of the *Dam15* mutation, and phage packaging and viability. We assessed complementation of *D::lysk* fusions in a variety of arrangements and components under fully repressed, partially derepressed and fully induced conditions and observed that the D_{wt} positive

control, as expected, was able to fully complement *Dam15* at the 37^{o} C ideal inducing temperature (Table 3). This plasmid served as the positive control for complementation. The plasmid expressing *D::eGFP* was previously shown to complement the *Dam15* mutation and as expected showed full complementation at 37° C. In contrast, the temperature-inducible plasmid backbone (pPL451) is devoid of *D*, serving as the negative control, and as expected, could not restore viability at any temperature. Within these controlled parameters we next sought to determine the ability of our *D::X* constructs integrated into this expression system, to complement for the *Dam15* mutation, thereby directly assessing the ability of gpD to maintain functionality in the fusion.

As expected, all fusions provided minimal complementation under repressed (30^{o} C) conditions, posting plating efficiencies that are likely due to genetic reversions of *Dam15*. Surprisingly, however, under induced conditions all the D::X fusions repeatedly performed poorly in complementation assays only improving viability from less than 100 to 500-fold compared to the negative control. In contrast, the positive control restored viability by greater than 10^{5} fold. The worst performer of the experimental fusions was the CHAP::D::SH3 construct, which possessed fusions to both the amino (CHAP domain) and carboxy (SH3) termini of gpD, and restored viability only 10-fold compared to repressed conditions, and 100-fold compared to the negative control. In isolation, fusion to N- versus C-terminal did not appear consequential as CHAP::D (N-terminal) and D::CHAP offered similar restoration to the *Dam15* phage under induced conditions. Based on repressed temperature viabilities of

all constructs, leakage of the promoter under repressed conditions appears likely. We did try to further improve repressor activity by conducting plating assays at 25^{o} C. No plaques were visible at this temperature indicating full repression, but confluence of bacteria on the plate was low at high phage, indicative of cell killing.

Table 3. Complementation of the infecting λ *Dam15* mutation by inducible D::X genetic fusion constructs in a non-suppressor strain.

Inducible Gene(s)	Plasmid[1]	Efficiency of Plating (e.o.p)[2]			
		25° C	30° C	35° C	37° C
N/A	None	np	$<2.3 \times 10^{-7}$	$<6.1 \times 10^{-7}$	$<5.0 \times 10^{-7}$
None	pPL451	np	$<7.7 \times 10^{-8}$	$<6.0 \times 10^{-7}$	$<3.7 \times 10^{-7}$
D::eGFP	pKS1	nd	7.5×10^{-6}	2.0×10^{-5}	0.02
D::CHAP	pEF-2	np	2.0×10^{-6}	5.4×10^{-5}	1.0×10^{-4}
CHAP::D	pEF-3	np	8.0×10^{-6}	2.8×10^{-5}	1.4×10^{-4}
D::SH3	PEF-5	np	1.6×10^{-5}	5.6×10^{-5}	5.0×10^{-5}
CHAP::D::SH3	pEF-6	np	4.6×10^{-6}	3.0×10^{-5}	3.9×10^{-5}
D::Bind	pEF-4	np	7.0×10^{-6}	8.7×10^{-5}	1.1×10^{-4}
D::LysK	pEF-1	np	1.6×10^{-6}	6.8×10^{-5}	6.8×10^{-5}
D_{wt}[3]	pPL451_D	np	6.7×10^{-6}	6.2×10^{-4}	8.0×10^{-1}

[1] W3101 strains harbour pPL451_X plasmids. pPL451 plasmids place downstream control of cloned gene(s) under the temperature-sensitive CI857 repressor. As temperature increases, CI857 activity is lost and gene expression increases.

[2] Plating efficiency of λF7 (λ*imm21Dam15)* on indicated strain/condition compared to that on BB4 (Sup^+) that was used as 100% control. E.o.p's are calculated as a ratio of experimental PFU/PFU on BB4 at that same temperature. E.o.ps are averages based on a minimum of two trials.

[3] D_{wt} is wild type gpD

nd, not done

np, no plating

In the attempt to overcome the observed recalcitrance of our fusions' incorporation into the phage capsid, we next investigated whether the *D::X* fusions could effectively complement the λ*Dam15* mutation in a suppressor strain derivative. SupD is a W3101 isogenic derivative that imparts the insertion of a serine residue at the 68th position instead of the programmed stop encoded by the *Dam15* mutation, thereby circumventing the premature stop and protein truncation. SupD confers a gpDQ68S allele that offers poor capsid functionality, but was previously shown to maximize fusion incorporation of gpD::eGFP when combined *in vivo*. We assessed the ability of the (strain) gpDQ68S / *D::X* (plasmid) combination to complement λ*Dam15*, indicating the degree of D-mediated stability of the resultant phage (Table 4).

Table 4. Complementation of the infecting λ *Dam15* mutation by inducible D::X constructs in a suppressor strain.

Inducible Genes	Plasmid[1]	Efficiency of Plating (e.o.p)[2]			
		25 °C	30 °C[3]	35 °C	37 °C
None	pPL451	np	$<7.14X10^{-8}$	$<1.61X10^{-8}$	$<1.63X10^{-7}$
D::CHAP	pEF-2	np	$<2.32X10^{-1}$	$2.01X10^{-1}$	$2.02X10^{-1}$
CHAP::D	pEF-3	np	$<2.74X10^{-1}$	$1.99X10^{-1}$	$2.05X10^{-1}$
D::SH3	pEF-5	np	$<3.94X10^{-1}$	$2.01X10^{-1}$	$2.56X10^{-1}$
CHAP::D::SH3	pEF-6	np	$<4.14X10^{-1}$	$1.49X10^{-1}$	$2.20X10^{-1}$
D::Bind	pEF-4	np	$<5.06X10^{-1}$	$2.31X10^{-1}$	$2.81X10^{-1}$
D::LysK	pEF-1	np	$<2.39X10^{-1}$	$2.56X10^{-1}$	$1.97X10^{-2}$
D_{wt}[4]	pPL451_D	np	$<5.45X10^{-1}$	$3.70X10^{-1}$	1.0

[1] W3101 strains harbour pPL451_X plasmids. The pPL451 plasmids place downstream control of cloned gene(s) under the temperature-sensitive CI857 repressor. As temperature increases, CI857 activity is lost and gene expression increases.

[2] SupD strains harbour pPL451_X plasmids. All efficiencies were compared to that on BB4, an *E. coli* strain with two suppressor mutations that allows 100% plating of λF7. E.o.p was calculated by determining the ratio of plaques forming units (PFU/PFU) of experimental strain and BB4 at either of the experimental temperatures. E.o.p's are the average based on a minimum of two trials.

[3] Plaques were extremely small and pinpoint and accurate counting was not possible, although at high concentrations, lysis was observed.

[4] D_{wt} wild type gpD

np, no plating

The SupD strain carrying the pPL451 (D-) plasmid was unable to suppress the λ*Dam15* mutation at all tested temperatures due to the poor functionality of the gpDQ68S allele and the absence of *D::X* complementation. In contrast, the positive control plasmid expressing *D* was able to fully complement *Dam15* at the fully derepressed temperature of 37° C, increasing phage viability by more than 10^4-fold compared to the fully repressed temperature of 25° C, where no plating was evident despite a weaker cell lawn, indicative of cell killing. Interestingly, at 30° C, evidence of lysis was obvious, but plaques were pinpoint and so small that lysis could only be detected when phage were plated at extremely high concentrations. Individual plaques could not be discerned at higher dilutions, making accurate e.o.p. calculations at these temperatures impossible. This finding indicates that some viable phage progeny are being assembled at even 30° C, but burst sizes are so small that individual plaques are not even visible. We scored plaques of this phenotype as negative, due to the inability to visually quantify, considering successful complementation as the ability to increase burst size to generate visible plaques. Upon shifting to 35° C, plaques were now discernible and plating efficiency was almost full for the positive D_{wt} control and complete at the fully derepressed temperature of 37° C.

All of the *D::X* fusion plasmids behaved similarly to that of the positive control. No λ*Dam15* plaques were visible at the fully repressed 25° C temperature and again, while lysis was evident even at 30° C, individual plaques were not discernible until 35° C, where *D::X* is partially derepressed. Under fully induced conditions, all *D::X* fusion complemented phage plated with relatively equal

efficiency at about a fifth to a quarter of the full efficiency seen on gpD^+ cells. These data indicate that the expression of all *D::X* fusions could, to some extent, complement and enhance suppression of λ*Dam15*.

Stability of phage displaying endolysin-capsid fusions.

We previously noted that gpD::eGFP decorated phage, either alone, or in combination with the gpDQ68S allele were more unstable in neutral solution (Nicastro et al., 2013). To ensure and assess the stability of phage displaying gpD::X endolysin capsid fusions we assayed the ability of resultant phage to tolerate EDTA. EDTA is a chelator of divalent cations and Mg^{2+} chelation would result in relaxation of phage DNA and added pressure on the phage capsid, busting structurally unstably phage. Phage displaying endolysin and its derivatives fusions were incubated with EDTA buffer following the standardized protocol, then assessed for degree of phage bursting as a result of Mg^{2+} chelation, by testing phage viability (Table 5).

Table 5. EDTA sensitivity of fusion phage grown in absence and presence of the gpDQ68S allele.

Plasmid[1]	Fraction Stability of EDTA-treated Phage[2]		
	Sup-	**SupD**	**Sup- / SupD**
D_{wt}	0.63 ± 0.28	-	-
D::eGFP	0.36 ± 0.15	0.59 ± 0.23	0.60
D::CHAP	0.96 ± 0.53	1.0 ± 0.94	0.41
CHAP::D	0.76 ± 0.02	0.48 ± 0.86	0.39
D::SH3	0.58 ± 0.11	0.85 ± 0.02	0.76
CHAP::D::SH3	0.90 ± 0.25	1.3 ± 0.11	0.60
D::Bind	1.9 ± 0.41	1.7 ± 0.59	1.1
D::LysK	0.96 ± 0.40	2.9 ± 1.20	0.28
None	0.85[3]	0.81	1.0

[1] pPL451 derivative (temperature-inducible plasmids).

[2] W3101, λ*imm21Dam15* phage grown on W3101 cells harbouring plasmids at optimal 37° C and e.o.p. represents EDTA-treated divided by untreated control. All stabilities are based on averages and have been repeated at least twice.

[3] λ*Dam15* here cannot grow on the Sup- strain and was grown on BB4 strain (Sup^+ strain that restores the gpD pristine sequence).

Phage λ*Dam15* was not severely impaired by EDTA, but did not demonstrate full stability, likely due to the low level of suppression by the SupE strain that cannot fully decorate and stabilize the capsid. Similar limited stability was noted for the control, gpD_{wt} complemented phage that exhibited mild viability impairment following EDTA treatment that was slightly improved in the presence of the gpDQ68S allele. As a reference, we show phage decorated by gpD::eGFP via both Sup- and SupD strains where decoration by gpD::eGFP alone is notably most sensitive, and 64% more stable in combination with the gpDQ68S allele.

The gpD::endolysin fusions ranged slightly in conferred stability with D::SH3 phage showing the greatest sensitivity. Interestingly, the full LysK (gpD::LysK) also possessing SH3 and fused in the same orientation to the C-terminal of D, showed very little impairment in either strain. The CHAP::D fusion phage indicated an interesting profile that was unlike all other fusions tested, in that the presence of this fusion's reduction of phage viability was 66% greater when combined with the gpDQ68S allele. In contrast, all other fusions, and even gpD_{wt} itself, reduced EDTA sensitivity when combined with the gpDQ68S allele. Given the impacts of SH3 C-terminal fusion and N-terminal CHAP fusion on phage viability, it was surprising to find that the CHAP::D::SH3 allele that possesses both of these fusions did not have any noticeable effect on phage sensitivity to EDTA, in solo and improved stability in combination with the gpDQ68S allele.

Variability between trials of some of the gpD::X endolysin fusion constructs was very large when assembled in combination with the gpDQ68S allele. The gpD::LysK, CHAP::gpD::SH3 and gpD::CHAP expressing phage varied remarkably in their sensitivity to EDTA, despite further repeated trials, varying from greater-than-wildtype stability to remarkably EDTA-sensitive. While e.o.p. assays are subject to considerable variability between assays, variance of this degree suggests a valid cause for the variability. This may be due to the presence of dual populations of phage that are formed during assembly of phage arising by the arrangement of trimers in the capsid.

Assessing the ability of endolysin-displaying phage to lyse S. aureus strains.

We next sought to determine whether our constructed gpD::X endolysin-decorated phage can confer lysis of various *S. aureus* strains for which the Phage K endolysin (LysK) is specific. We tested the lytic activity of the phage displaying endolysin and its derivative fusions on the λ*imm21Dam15* phage capsid; each was generated in isolation on the Sup- (gpD-), SupD (gpDQ68S) or SupE (D_{wt}) strains (Table 6). Due to the limited upper concentrations that could be generated by some of our lysate preparations, we standardized our phage lysates to 10^7-10^8 PFU/mL to appropriately compare their effect on target cell lysis. To assess lysis, phage preparations were added to a confluent lawn of clinically relevant strains of *S. aureus*, including MRSA, VRSA and bovine *S. aureus*. As this work represents the first attempt to construct a phage-based endolytic particle, a positive control for phage display lysis does not yet exist. As a comparator and a basis against which to qualitatively score lysis via each

phage preparation, we employed chloroform as a positive control. As negative controls we employed the phage suspension buffer medium as a medium control and λ*Dam15* phage prepared *via* complementation by plasmid D_{wt} as the phage display control.

Table 6. Assaying endolysin-displaying phage lysis of *S. aureus* strains.

gpD::X Fusion	Original Lysate Titer PFU/mL[1]			Lysis Activity on *S. aureus*[2]		
	Sup-	SupD	SupE	MRSA	VRSA	Bov. SA
None (Buffer)	N/A	N/A	N/A	—	—	—
D::CHAP	3.4×10^9	3.1×10^9	N/A	—	—	—
CHAP::D	9.0×10^9	2.5×10^9	2.1×10^9	—	—	—
D::SH3	7.5×10^9	1.4×10^8	1.8×10^9	—	—	—
CHAP::D::SH3	6.0×10^8	1.4×10^9	4.0×10^7	—	—	—
D::Bind	1.4×10^9	1.6×10^8	1.2×10^9	—	—	—
D::LysK	5.4×10^8	3.3×10^8	6.8×10^8	—	—	—
D_{wt}	7.5×10^9	7.5×10^9	2.6×10^8	—	—	—
$CHCl_3$	N/A	N/A	N/A	+++	+++	+++

[1]Original Sup- and SupD lysates were standardized to10^8 PFU/mL and SupE to 10^7 PFU/mL before testing.

[2] Lytic activity was measured by adding 10^5 of SupE and 10^6 of Sup- and SupD phage to a lawn overlay of target cells and scored according to $CHCl_3$ lysis, used as a complete lysis positive control.

As expected, none of the negative controls lysed any of the tested *S. aureus* strains at the standardized or unstandardized concentrations. And, surprisingly, we did not observe any notable lysis for any of the gpD::endolysin fusion phage. We did expect to see lysis with the phage displaying the catalytic domain fusions such as gpD::CHAP, CHAP::gpD, catalytic domains and specificity domains such as gpD::Bind and CHAP::gpD::SH3 and the fully displayed endolysin gpD::LysK, but lysis was not evident in any of the administered displayed phage constructs. Phage displaying D::SH3 also displayed no lytic activity, as expected, since the domain SH3 only encodes the specificity domain. We also tested displayed phage generated from SupD (gpDQ68S) and SupE (gpD_{wt}) suppressor strain backgrounds to try and address the possibility that the lack of phage activity might be due to poor incorporation in the absence of gpD_{wt} or another wild-type length allele and improve incorporation. However, as with Sup- phage preparations, lysis was also not observed for phage derived from any of the suppressor strains. At this point, we reasoned that the lack of observed lysis may be due to either inadequate expression of fusions per phage, too few phage, or loss of lytic functionality of LysK lytic domains upon fusion with gpD, or a combination thereof.

Assessing the functionality of isolated gpD::X endolysin fusion derivatives.

Upon noting that endolysin-displaying phage were not functional in lysing the desired *S. aureus* target strains, we asked whether the isolated gpD::X endolysin fusions themselves possessed lytic activity in the absence of the phage or phage capsid. To initiate this investigation each *D::X* fusion sequence was first cloned

into the high efficiency expression vector pET30a+ to express, purify and test the cloned fusion inserts for lytic functionality. All fusion inserts were excised from their parent (pPL451) inducible vectors and successfully cloned into the MCS of pET30a+ His-tagged high efficiency expression vector. The resultant chimeric vectors were analyzed and confirmed by endonuclease digestion, and size of the insert following agarose gel electrophoresis (AGE; Figure 7).

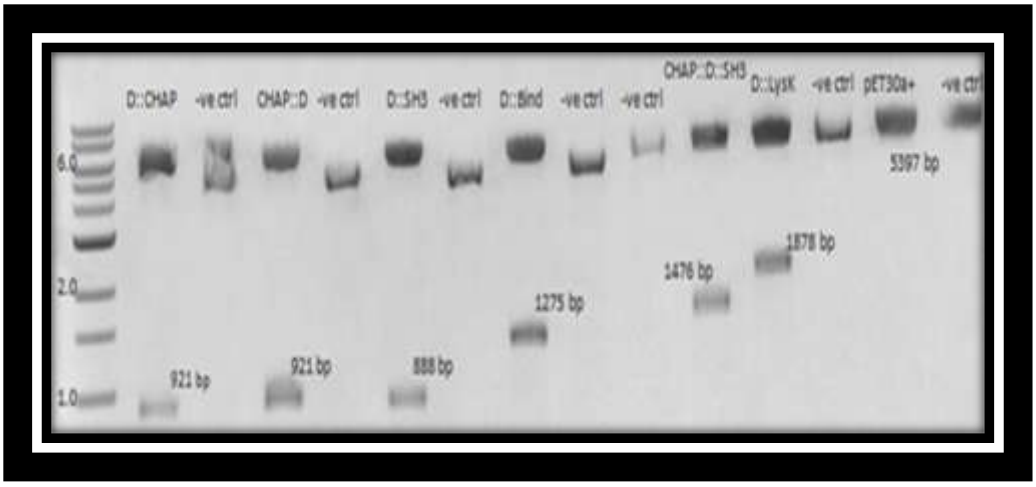

Figure 10. Cloned endolysin *D::X* fusions into the high efficiency His-tagged expression vector, pET30a+. Successful cloning of D::lysk and the other domains into expression vector pET30a+ MCS. The band sizes are labelled next to their respective bands. The expression vector, pET30a+, was digested with restriction enzymes (BamHI and HindIII) to facilitate the ligation of the D::X endolysin fusions which were also digested with the same enzymes to produce compatible ends. Inserts and their expected band sizes are: D::CHAP, 921 bp, CHAP::D, 921 bp, D::SH3, 888 bp, D::Bind, 1275 bp, CHAP::D::SH3, 1,476 bp and D::lysK, 1,878 bp.

The pET30a+ vector, a plasmid of 5,397 bp, was cut with the same restriction endonucleases as that of the inserts and was prepared and analyzed alongside the experimental clone indicating, in each case, a lack of any additional bands as was seen upon digestion of each endolysin *D::X* plasmid clone. As a positive control for subsequent experiments, *lysK* (encoding wild type LysK), was also cloned and analyzed in the same manner (Figure 8).

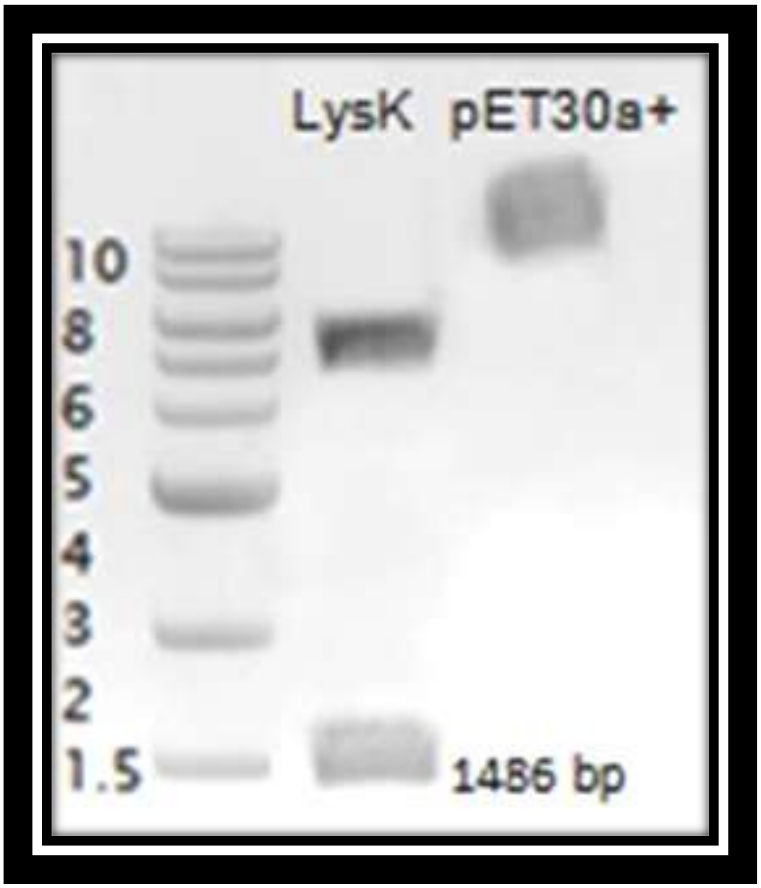

Figure 11. Cloned lysK in a high efficiency His-tagged expression vector. The lysK gene was successfully cloned into pET30+ with a fragment size of 1,486 bp. The positive control, lysK, and pET30a+ were digested with KpnI and HindIII restriction enzymes to produce compatible ends for ligation.

Total protein was extracted from induced cultures of each clone to preliminarily assess functionality of all fusion proteins in regards to lysing and killing target *S. aureus* cells. First, a standardized amount of each crude protein lysate was added to a fresh lawn of live and dead (autoclaved) bovine *S. aureus*, MRSA and VRSA to assess the lytic activity of each protein fusion (Figure 9; Table 7).

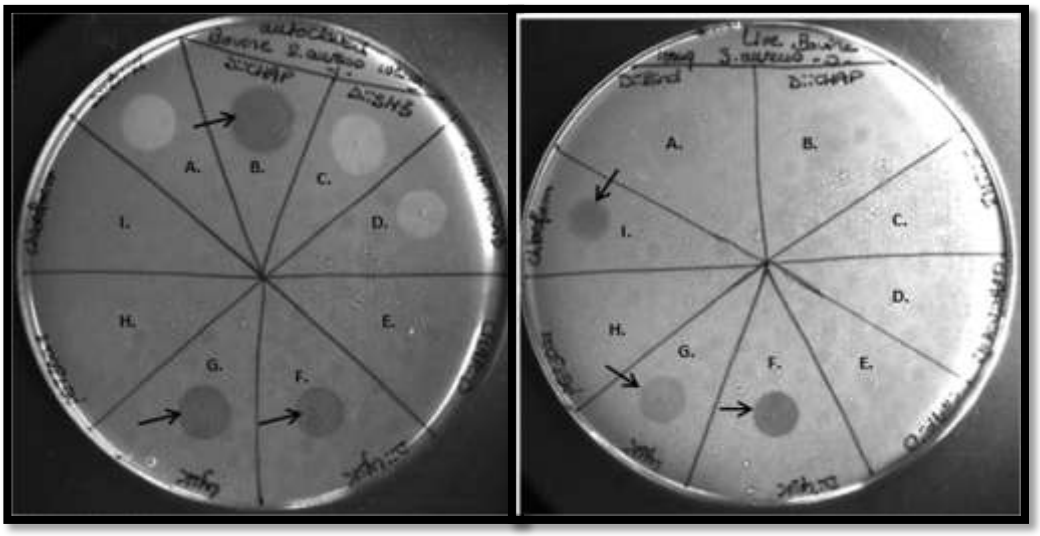

Figure 12. Zymogram lysis assay with standardized gpD::X endolysin protein challenge. Left plate= dead (autoclaved), right plate= live. A. gpD::Bind, B. gpD::CHAP, C. gpD::SH3, D. CHAP::gpD::SH3, E. CHAP::gpD, F. gpD::LysK, G. LysK, H. pET30a+, I. Chloroform. A total crude protein lysate of 100 μg was added to fresh bovine *S. aureus*. Lysis assay was repeated three times with identical results. Arrows indicate detected lysis spot.

Table 7. Endolysin gpD::X fusion protein lytic activity on bovine *S. aureus.*

gpD::X Fusion Protein[1]	Lytic Activity[2]	
	Live cells	**Dead cells**
None (Buffer)	—	—
LysK	++	++
gpD::LysK	+++	++
gpD::CHAP	—	++
CHAP::gpD	—	—
gpD::SH3	—	—
CHAP::gpD::SH3	—	—
gpD::Bind	—	—
$CHCl_3$	+++	—

[1] Total protein added was100 µg

[2] Includes at least 3 repeated tests on bovine *S. aureus.*

Wild type LysK, serving as the positive control, exhibited strong lysis on both live and dead (autoclaved) bovine *S. aureus* cells. Chloroform $CHCl_3$ was used as a comparator in this assay as well, exhibiting lysis on only live cells of bovine *S. aureus*, as expected, but no effect on dead cells. Chloroform did not show any lytic activity on dead bovine *S. aureus* cell lawn as it disrupts the bacterial cell membrane by permeabilizing it and since bacterial cells undergo a physiological change of the membrane through disruption of cell membrane when subjected to high temperature and pressure, chloroform would deem inactive in lysing cells (Manning & Kuehn, 2011). From the experimental gpD::X endolysin fusion proteins, only gpD::LysK exhibited lytic activity on both live and dead *S. aureus*

cells, whereas gpD::CHAP exhibited activity on dead *S. aureus* cells only, in all cases, lytic activity was detected within 3 h after incubation. None of the other protein fusions showed any noticeable lytic activity on either living or dead bovine *S. aureus.*

To more quantitatively determine the lytic activity of LysK endolysin and the derivative gpD::X fusions, we performed inhibitory concentration assays on bovine *S. aureus* in order to assess the concentration ranges within which, the endolysin fusions could prevent growth of target cells. Protein was added at standardized levels to bovine *S. aureus* and ascertained for cell killing ability (Figure 10; Table 8). As expected, the parent expression plasmid pET30a+ (negative control) showed no lytic activity at all tested concentrations. In contrast, purified LysK (positive control) exhibited a powerful killing effect, reducing viable cell titers by $>10^3$-fold at all applied doses, compared to the plasmid control. Interestingly, LysK was out-competed by the gpD::CHAP. In general, constructs harbouring the catalytic CHAP domain (gpD::CHAP, CHAP::gpD and gpD::LysK) exhibited varying degrees of lytic activity, with the exception of CHAP::gpD::SH3 that offered no lytic activity, likely due to compromised folding of the protein. Similarly, no killing or even enhancement of lytic activity was observed by gpD::Bind, nor by the non-catalytic specificity gpD::SH3 domain fusion, as was expected. The gpD::CHAP

fusion exhibited the strongest killing activity that was 10^4 fold greater than the plasmid negative control, followed by gpD::LysK fusion that offered the second greatest killing profile that although 100-fold greater than the control, was more

than 100-fold lower than gpD::CHAP and 10+-fold lower than wild type, LysK. Interestingly, CHAP::gpD imparted the lowest killing activity, offering 10^3 lower lytic activity than its conformational counterpart, gpD::CHAP. Finally, as expected, the specificity domain gpD::SH3, did not elicit any lytic activity at all tested concentrations.

Table 8. Inhibition of target cell growth by gpD::X protein lysates on bovine *S. aureus.*

Protein Lysate	Protein Addition (µg)		
	7.5	**15**	**37.5**
pET30a+	1.0*	1.0	4.5×10^{-1}
D::CHAP	$<1.9 \times 10^{-5}$	$<1.9 \times 10^{-5}$	$<1.9 \times 10^{-5}$
CHAP::D	4.7×10^{-2}	3.1×10^{-2}	2.0×10^{-2}
D::SH3	1.0*	1.0	1.0
CHAP::D::SH3	1.0	1.0	1.0
D::Bind	1.0	1.0	1.0
D::LysK	3.8×10^{-4}	$<1.9 \times 10^{-5}$	$<1.9 \times 10^{-5}$
LysK	2.1×10^{-4}	$<1.9 \times 10^{-5}$	3.8×10^{-5}

*Values slightly greater than 100% were still listed as 1.0. Experiment was repeated at least twice.

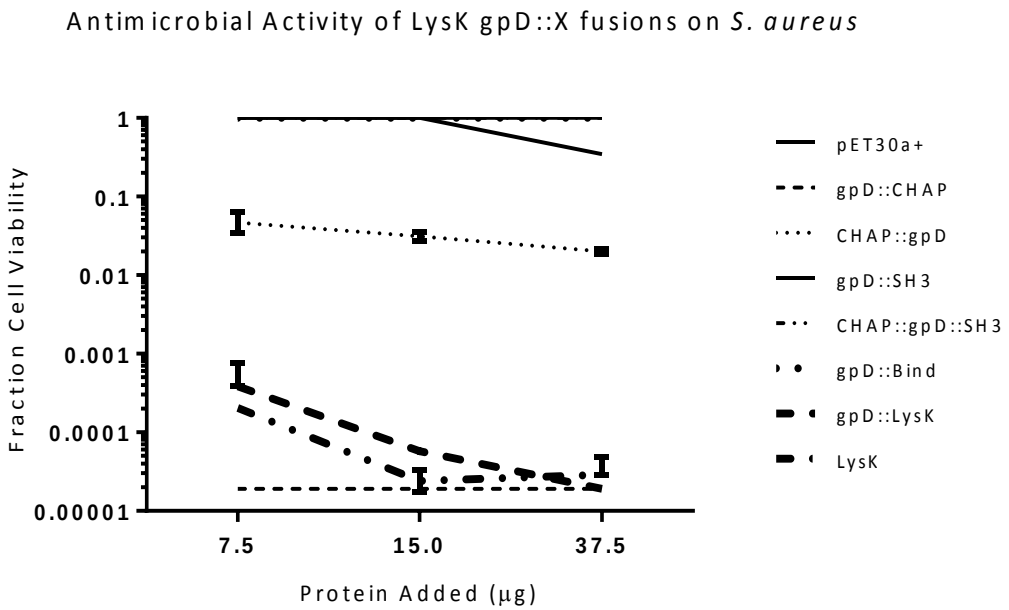

Figure 13. Antimicrobial activity of LysK gpD::X fusions on *S. aureus*. All gpD::X endolysin fusion proteins were purified via a His60 Nickel column and tested each lysate for and the presence of His-tagged gpD::LysK, gpD::CHAP, CHAP::gpD, gpD::Bind, CHAP::gpD::SH3, gpD::SH3 or LysK protein by SDS-PAGE gels (Figure 11A-G). In each case, pET30a+ served as the negative control. In all protein purifications, the primary species is identified. Cell protein contamination occurred to varying degrees in preparations, with poorest purification and greatest fractional contamination obvious for CHAP::gpD::SH3. This finding may be due to the poor translation of this protein, subjecting it to proteolytic degradation. It is worthy to note that gpD::SH3, gpD::Bind and CHAP::gpD::SH3 lines overlap.

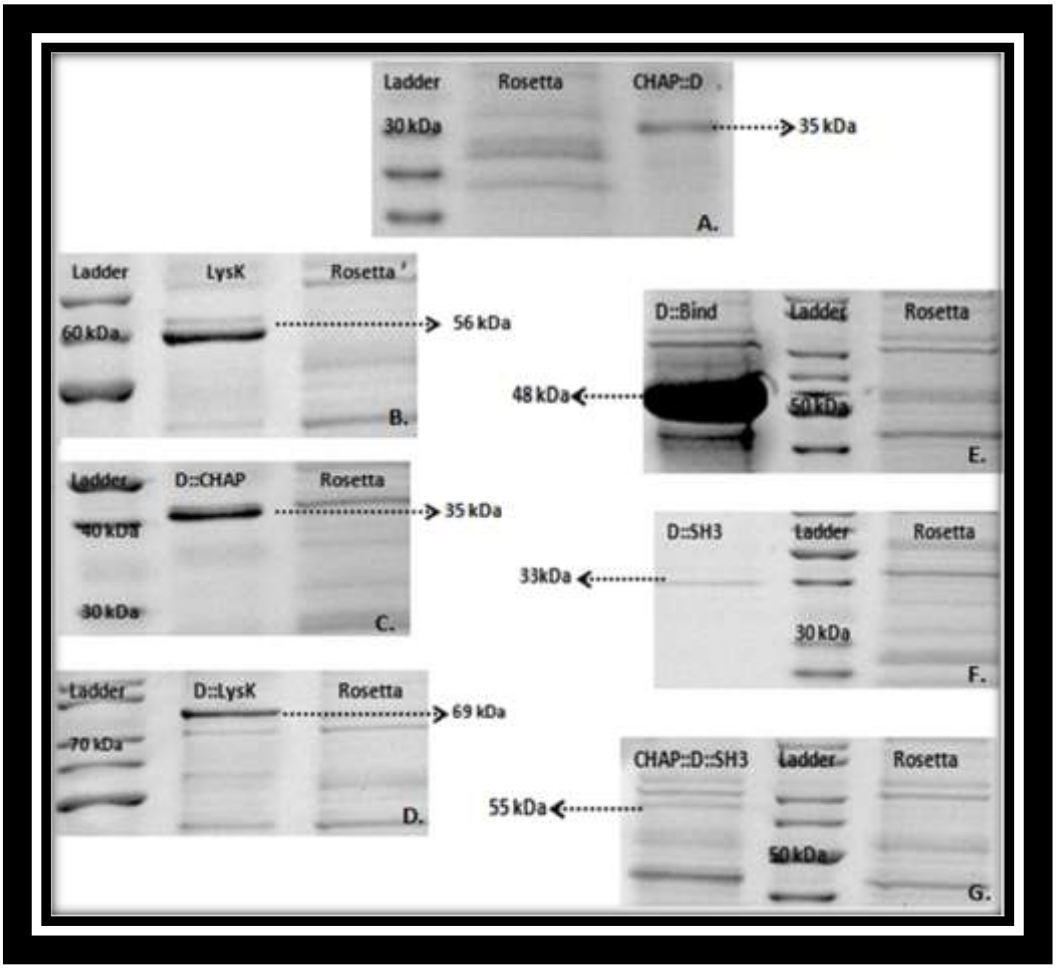

Figure 14. SDS-PAGE images of purified gpD::X endolysin fusions. A. CHAP::D, B. LysK, C. D::CHAP, D. D::LysK, E. D::Bind, F. D::SH3, G. CHAP::D::SH3. Each figure contains protein molecular weight marker (ladder), 4 μg of the purified protein and whole Rosetta cell lysate without plasmid (cell's native proteins). A. CHAP::D band migrated closely to slightly higher than the expected size of 35 kDa. B. LysK band migrated slightly higher than the expected size of 56 kDa. C. D::CHAP band migrated slightly higher than the expected size of 35 kDa. D. D::LysK band migrated higher than the expected size of 69 kDa. E. D::Bind band migrated very closely to the expected size of 48 kDa. F. D::SH3 band migrated higher than the expect band size of 33 kDa and finally, G. CHAP::D::SH3 band migrated slightly higher than the expected band size of 55 kDa.

Chapter 5: Discussion

While other surface display systems have been developed such as microbial cell systems in *E. coli,* yeast cell systems like *Saccharomyces cerevisiae* and eukaryotic cell systems like human embryonic kidney cells, the use of phage for surface peptide display remains the preferred approach (van Bloois et al., 2011; Lee et al., 2003; Kondo & Ueda, 2004; Ho & Pastan, 2009). The main advantages of phage display include the abilities to express a vast variety of fusions on the different phage elements and flexibility in designing phage screening assays (Willats, 2002). The display of proteins on phage λ capsid also eliminates the need for large-scale production and purification of recombinant proteins which is often a costly and tedious procedure. As a primary candidate for lytic phage display, λ is capable of incorporating up to 405-420 copies of the major capsid protein (gpD), the major capsid protein that has been extensively exploited for the display of foreign proteins (Nicastro et al., 2013, Nicastro et al., in press, Casjens & Hendrix, 1974). The trimeric nature of gpD enables a dual display fusion on its N and C termini, hence maximizing the number of displayed proteins (Nicastro et al., 2013; Sternberg and Hoess, 1995). Recently, Nicastro et al. (2013) developed a phage λ system by exploiting a dual genetic control mechanism to display foreign proteins on phage λ capsid in a variable manner. The degree of decoration of foreign proteins on the phage capsid is controlled by both temperature-sensitive regulation of expression of the fusion in conjunction with variable functionality of gpD alleles generated by various engineered host strains. The level of decoration on the phage capsid can be

effectively controlled through the modification and regulation of the two controllable elements.

In this study, we sought to design, construct and characterize λ-based display particles by way of generating translational fusions to the C-terminal and/or N-terminal of gpD. We constructed and assessed the lytic activity of different fusion arrangements of LysK and its domains on the decorated phage capsid, or as purified gpD::X domain (gpD::LysK, gpD::CHAP, CHAP::gpD, gpD::Bind, gpD::SH3, CHAP::gpD::SH3) proteins. From the published applications of phage λ display to date, there are no studies to our knowledge that report the display of functional lytic proteins on λ capsid for antimicrobial purposes. While some of the constructs were able to complement for the *Dam15* mutation in Sup- cells, this complementation was generally 10^4-fold lower than that of D_{wt} at induced temperatures. This is most likely explained by the poor formation of gpD homotrimers, which is a prerequisite for proper capsid formation as not all fusions are well tolerated. Termed "recalcitrant" such fusions prevent protein oligomerization and the formation of gpD trimers during phage assembly and therefore display fewer D-fusion proteins. Hayes et al. (2010) in their construction of a circovirus vaccine, fused four immunodominant regions of the porcine circovirus capsid to the C-terminal of gpD (D-CAP), a second with GFP (D-GFP) and a third with SPA tag protein (D-SPA). While the D-GFP and D-CAP fusions could be expressed constitutively without compromising the viability of the host, D-SPA expression reduced the viability of the cell by >50-fold thus not all fusions are well tolerated.

By controlling the level of fusion protein production, particularly by supplementing with supplemental gpD allele(s), recalcitrance may be overcome, leading to the use of isogenic SupD that generates the gpDQ68S allele (serine) to supplement endolysin gpD::X complementation. As the gpDQ68S allele possesses poor functionality, λ*Dam15* mutants plated on this strain tend to form pin point plaques that cannot be seen in isolation, allowing for any complementation on this strain to be visualized and quantified by increasing plaque size. The physical representation of the plaques in SupD backgrounds changed from pin point plaques at lower temperatures to clear and larger sized plaques at higher temperatures where expression of the gpD::X was greatest. This finding suggests that the substitution of glutamine in the wild type gpD sequence with the smaller (105.1 Da) serine that is biochemically similar as a polar neutral amino acid is highly ineffective in the suppression of the *Dam15* allele. In the absence of complementing *D* allele expression effectively, the burst size associated with the lytic infection produces very few particles per host, thereby forming pin point plaques. Possible reasons for the dramatic effect of the serine substitution at residue 68 of gpD include interference in gpD trimerization and/or compromised interaction with gpE hexamers, although previous findings indicate that gpD N-terminus is located closer to the 3-fold axis of the gpD trimer (Yang et al. 2000) and may be involved with interacting with gpE. Our lab previously showed that phage decorated by the gpDQ68S allele are also about the third the size of wild type phage and highly unstable,

suggesting that the incorporation of this allele into the capsid is much lower than gpD_{wt} (Nicastro et al., 2013).

The lowest level of complementation was observed for the CHAP::D::SH3 fusion. In addition to recalcitrance that plagued all endolysin fusion constructs, the lack of complementation for this construct may additionally be attributed to the size of the resultant protein. Yang et al., (2000), concluded that the fusion of large proteins to the termini of gpD decreased the complementation and hence viability of decorated phage particles. In line with this inference, we similarly noted poor complementation by the gpD::LysK fusion, which is even larger (621 a.a, ~ 68 kDa), suggesting that size does play a role in limiting decoration and viability. Gupta et al. (2003) found that a peptide of 72 a.a (~7.9 kDa) had 350 copies incorporated on the phage capsid in comparison to a 231 a.a (~ 25 kDa) peptide that had 154 incorporations, hence suggesting that as peptide length increases its display efficiency decreases. The display of lytic proteins on the λ capsid is clearly far more complicated than the display of short peptides used for eliciting humoural responses or screening libraries. One of the limitations that could render LysK and its domains inactive on λ capsid may in fact be the improper folding of large proteins such as D::LysK.

The CHAP::gpD::SH3 construct also represents the first evidence to our knowledge of attempting to exploit both the amino and carboxy termini of each gpD *in tandem.* Vaccaro et al., (2006) were able to fuse scFv anti-CEA, which is a fairly large protein of 33.6 kDa (Rodenburg et al., 1998), to either of the N and C termini of gpD, but not *in tandem*. It is likely that the CHAP::gpD::SH3 dual

fusion interferes with gpD folding and imparts very poor structural functionality. This inference is further supported by the finding that the purified protein also showed no lytic activity, suggesting that both gpD and the CHAP domain were non-functional. Pavoni et al., (2013) tested the ability to fuse anti-CEA scFv and GFP to gpD termini and express each simultaneously, similarly finding that this yielded unstable fusions which soon released the fused GFP from λ capsid. Although the C terminus construct had more fusions of scFv than the N terminus, only few plaques were generated indicating a reduced viability with the gpD dual termini fusions. It was also observed that there was a competition between the display of fusions on gpD termini and phage particle formation and more than often it was favoured to produce more phage particles with truncated fusion proteins than unstable phage λ capsids. This could explain why our dual fusion construct CHAP::gpD::SH3 generally had poor complementation. Pavoni et al., (2013) further studied and developed the λ display system of gpD fusions and were able to enhance the viability of plaques bearing C termini fusions of gpD by introducing amber mutants through BB4 (Sup^+) host strain.

We noted that the SupD (Sup^+) background strain when used for decoration of phage by gpD::X was more efficient in yielding functional gpD::LysK and its domains than on the Sup- strain. Previous studies similarly reported that low yields and decreased phage viability are associated with greater expression of capsid-fusion protein, although at the time they could not be sure that this observation was due to impaired capsid assembly (Mikawa et al. 1996; Maruyama et al. 1994). This finding is also in accordance with Nicastro et al.

(2013) who noted that the decorative capacity of gpD::eGFP on the phage surface was highest in combination with the gpDQ68S allele. They propose that the gpDQ68S allele stabilizes the gpD::eGFP fusion, and while neither possesses full gpD functionality (compared to D_{wt}), collaboratively, gpDQ68S-gpD::eGFP- gpDQ68S, or gpD::eGFP- gpDQ68S-gpD::eGFP intragenic (within gene) complementation is better incorporated than either allele alone (Nicastro et al. 2012).

With respect to stability, we found that fusions that would introduce larger protein constructs into the phage, such as CHAP::gpD::SH3, gpD::Bind, and gpD::LysK seem to be more stable than the smaller protein constructs like gpD::CHAP, CHAP::gpD and gpD::SH3. In combination with the complementation data, this is likely due to the fact that these fusions are not readily integrated into the phage capsid in the first place and as such carry only the supplemental gpDQ68S allele. Conversely, the combination of the gpD::X fusion with the gpDQ68S allele may in fact stabilize the capsid more than either alleles can accomplish on their own, resulting in greater resistance to EDTA. Of great interest, is the consistent variability in EDTA sensitivity that was observed for gpD::LysK, CHAP::gpD and gpD::CHAP decorated phage. We propose that this is due to the high degree of structural instability in the phage. Nicastro et al. (2013) noted that SupD fusions of gpD::eGFP had a great degree of variability in size and stability, proposing that this was due to an "all-or none" phenomenon of decoration when gpDQ68S was combined with the gpD::eGFP fusion. While assembled, phage may be adequately resistant to EDTA, structural instability

may lead to a disassembly from the phage, resulting in a domino effect, rendering the phage highly susceptible to EDTA and capsid bursting. As a result, EDTA sensitivity may be variable over time due to the presence of both decorated and undecorated populations.

We found that all phage decorated by gpD::LysK and LysK domains showed no lytic activity on bovine *S. aureus*, MRSA or VRSA. This was not too surprising as complementation was dramatically hindered by recalcitrance, imparting poor decoration of endolysin and its domains on the phage capsid. While we were hopeful, that some SupD-hosted phage would exhibit lysis on target cells, since it did appear to readily complement several of the D::X fusions, we noted no lytic activity of gpD::LysK and its domains decorated phage on *S. aureus*. The most likely explanation is that we are not adequately decorating the phage, and due to limited complementation, are not purifying displayed phage in adequate concentration. Another possible explanation is steric hindrance or size constraints. The thick peptidoglycan layer of *S. aureus* must be completely penetrated in order to lyse and kill the target cell. A highly decorated phage may range in the area of several hundred nm in diameter (Nicastro et al., 2013) and as such may not be able to adequately reach the deep amide bonds in the peptidoglycan layer despite effective hydrolysis of surface substrates.

Proper protein folding of integrated fusions in the phage capsid may also be compromised upon incorporation. Hayes et al. (2010) found that although they were able to integrate their porcine vaccine constructs into a λ display particle (LDP), LDP-D-GFP and LDP-D-SPA did not induce a useful antibody response

in vivo. Finally, it is possible that given the low complementation rate we were actually selecting for truncated fusions to incorporate into the phage head. Vaccaro et al., (2006) observed that one to five percent of plaques generated by C-terminal fusions were mutants possessing point mutations causing either frameshift or premature stop signals within the scFv gene, which suggests a powerful selection against the inefficient display of the antibody as a C-terminal fusion and the inhibitory effect on the assembly of viable phage.

To determine whether the gpD::X endolysin fusion proteins were themselves disrupted for lytic activity, we purified the fusion proteins and assessed lytic activity on the *S. aureus* strains. In contrast to phage lysis assays, we noted that gpD::LsyK protein fusion, like LysK, exhibited detectable lytic activity on both live and dead bovine *S. aureus*. This finding indicates that the gpD fusion to the N-terminal catalytic domain does not hinder CHAP activity. Interestingly, gpD::CHAP on the other hand, showed lysis on killed *S. aureus* only, indicating either that lytic activity is only possible on live cells in the presence of the attachment (SH3 domain), or the combination of cysteine and histidine dependent amino hydrolase (CHAP) and amidase-2 (Bind) domains are required to impart this phenotype; this is a new finding.

Mattiacio et al., (2011) found that a soluble peptide, gp140, was able to induce higher HIV-1 Env-binding antibody titers than the gp140 decorated on phage λ, thus restating the hurdles that Zanghi et al., (2005) and Hayes et al., (2010) faced for recalcitrance of the displayed proteins on phage λ capsids. The number of gp140 displayed fusions was 30 copies and that was far less than the expected

number of 405-420 copies that corresponds to the number of gpD copies on the phage λ capsid (Mattiacio et al., 2011). The possibility of displaying very few fusions on phage λ capsid may explain the undetectable lytic activity that we have observed in our phage constructs. In addition, Yang et al., (2000) found that gpD exists as a monomer in solution, in which they explained why gpD::X fusions exhibited greater functionality in solution than on the phage head. This inference agrees well with our qualitative and quantitative bovine *S. aureus* inhibition assays that showed variable protein gpD::LysK and gpD::CHAP lytic activities in contrast to the decorated phage particles. Although we did originally expect to observe lysis by CHAP::gpD::SH3 and CHAP::gpD constructs, it is possible that the fusion disrupted the folding of the CHAP domain. Pavoni et al. (2013) similarly found that eGFP fusion to the N terminal of gpD resulted in improper folding of eGFP hence jeopardizing its activity. Vaccaro et al. (2006) additionally found that incorporation of N terminal fusions to gpD was 38% lower than C terminal fusions (Vaccaro et al., 2006). MRSA and VRSA were not efficiently lysed by any of the protein fusions; this is in agreement with the findings of Horgan et al., (2009) and O'Flaherty et al., (2005) who both found that LysK exhibited weak lytic activity on these strains with maximal lytic affect seen on bovine *S. aureus*.

We did not observe any lytic activity for the purified protein fusions on bovine *S. aureus*, MRSA and VRSA. This could be due to the composition of the protein buffer suspension that may have played an important role in reducing the functionality of the eluted protein fusions. Fenton et al., (2011) observed that a

300 mM concentration of NaCl tremendously decreased the activity of CHAP peptidase. Our elution buffer necessary for eluting off of Nickel column was similarly composed of 300 mM of NaCl that may have further compromised activity. The presence of high imidazole concentrations (300 mM) may have also interfered with protein activity by forming aggregates (Sharma et al., 1992). Finally, the 6xHis tag sequence to the N-terminal of fused protein has been shown to interfere with protein folding (Hefti et al., 2001); this may have altered the folding, reducing catalytic activity of the CHAP domain.

We performed growth inhibition assays as a more sensitive and quantitative approach to assess the antibacterial activity of gpD::X protein fusions. The results of these assays generally agreed with the qualitative zymogram test results, showing that gpD::LysK, gpD::CHAP and positive control, LysK all had varying degrees of lytic activity on bovine *S. aureus*. The results from the zymogram and inhibition assays confirm that CHAP peptidase is able to effectively cleave the peptidoglycan bonds of bovine *S. aureus* as a soluble monomer, suggesting again that the lytic activity of each of gpD::LysK and gpD::CHAP is likely compromised when displayed on phage λ capsid. The finding that CHAP::gpD exhibited milder antibacterial activity in the inhibition assay, but not in the crude protein lysate zymogram assay, may be explained by increased sensitivity of the former assay.

The lytic activity of the CHAP peptidase that was observed in each of the crude lysates of gpD::LysK, gpD::CHAP and CHAP::gpD constructs can be backed up by extensive studies that were performed on it. A more recent published study

demonstrated the strong ability of LysK peptidase domain, CHAP, to eliminate biofilms caused by bovine *S. aureus* strains (Fenton et al., 2010). The biofilms were eliminated within 4 h following treatment and never grew back (Fenton et al., 2010). CHAP peptidase was observed to be more lytic protein than the amidase catalytic domain (Fig. 2), and that would explain why our gpD::Bind construct did not elicit any lytic activities on any of the staphylococcal strains tested.

As expected, gpD::SH3 construct, which is the peptidoglycan cell wall binding domain, did not show any lytic activity in either of the lysis assays performed. This agrees with the results of Becker et al. (2009) who did not observe any lytic clearing by purified SH3 domain. However, they did note that when SH3 was fused to CHAP domain (removed Bind domain), the lytic activity was comparable to wild type LysK activity. Our construct, CHAP::gpD::SH3 similarly resembles this construct, but the presence of gpD separating these two domains completely abrogated lytic activity (in addition to severely compromising gpD functionality), suggesting that misfolding or steric hindrance may have interfered with the catalytic activity of CHAP in the CHAP::gpD::SH3 construct.

Future Directions

Mosaic display of complemented gpD and gpD::X fusions is an approach that Zanghi et al., (2005) showed to enhance the incorporations of fusions on λ capsid and hence functionality. Here we have tested incorporation of fusions, supplemented by gpDQ68S. Other alleles, such as gpD_{wt} or gpDQ68Y alleles that confer far greater functionality may be preferable to improve incorporation. Recalcitrance may also be resolved by reducing expression of the *D::X* fusions during phage production by growing up the cells at a lower temperature (35^{o} C). Spacer size may also play an important role in improving gpD functionality and incorporation of fusions into the capsid, since it has been previously noted that a spacer increase from 10 to 92 a.a. can increases protein activity by 10-fold (Lee et al., 2003; Strauss & Götz, 1996).

Conclusion

In this study, we attempted to display phage K, endolysin K on the capsid of phage λ through translational fusions to the major capsid protein gpD. Fusion proteins were subject to strong recalcitrance and resultant phage display particles did not elicit any lytic activity on the tested clinically relevant *S. aureus* strains. The inactivity of the displayed fusions may be attributed to poor incorporation of fusions, steric hindrance or misfolding of proteins, or any combination thereof. Although some of our constructs were attempts to be dual fusions of gpD, literature and our findings suggest that fusion to the C terminal of gpD is a far better fusion in producing functionally lytic proteins (as seen in our soluble protein constructs). We further showed that the fusion of gpD to endolysin K (LysK) and CHAP does not dramatically interfere with CHAP catalytic activity as gpD::LysK, gpD::CHAP and CHAP::gpD showed variable antibacterial activities. Our findings disprove the original hypothesis, but answer essential questions and provide important new information toward improving gpD::LysK phage display and resolving protein fusion recalcitrance. Although this study is preliminary in designing and characterizing lytic proteins on phage λ capsid, it offers the promise that by enhancing the display of fusion proteins on phage capsid, functionally lytic decorated phage particles can be generated.

References

Browder, P., Young, J.R., Johnson, M., 1965. Lysostaphin: Enzymatic mode of action. Biochem. and Biophys. Res. commun. 19, 383–389.

Borysowski, J., Weber-Dabrowska, B., Górski, A., 2006. Bacteriophage endolysins as a novel class of antibacterial agents. Exp. biol. and med. 231, 366–377.

Becker, S.C., Foster-Frey, J., Donovan, D.M., 2008. The phage K lytic enzyme LysK and lysostaphin act synergistically to kill MRSA. FEMS microbiol lett. 287, 185-191.

Becker, S.C., Dong, S., Baker, J.R., Foster-Frey, J., Pritchard, D.G., Donovan, D.M., 2009. LysK CHAP endopeptidase domain is required for lysis of live staphylococcal cells. FEMS microbiol. lett. 294, 52-60.

Bratkovič, T., 2009. Progress in phage display: evolution of the technique and its applications. Cell. and mol. life sci. 3, 749-767.

Beghetto, E., Gargano, N., 2011. Lambda-display: a powerful tool for antigen discovery. Mol. 16, 3089-3105.

Chang, S., Sievert, D.M., Hageman, J.C., Boulton, M.L., Tenover, F.C., Downes, F.P., Shah, S., Rudrik, J.T., Pupp, G.R., Brown, W.J., Cardo, D., Fridkin, S.K. 2003. Infection with Vancomycin-Resistant *Staphylococcus aureus* containing the *vanA* Resistance Gene. N Eng. J Med. 348, 1342-1347.

Casjens, S.R., Hendrix, R.W., 1974. Locations and amounts of major structural proteins in bacteriophage Lambda. J. of mol. biol. 88, 535-545.

Cui, L., Murakami, H., Kuwahara-arai, K., 2000. Contribution of a Thickened Cell Wall and Its Glutamine Nonamidated Component to the Vancomycin Resistance Expressed by *Staphylococcus aureus* Mu50 Contribution of a Thickened Cell Wall and Its Glutamine Nonamidated Component to the Vancomycin Resistance E. Antimicrob. agents and chemother. 44, 2276-2285.

Canadian Antimicrobial Resistance Alliance. http://www.can-r.com/study.phphttp://www.can-r.com/study.php. Accessed on September 2013.

Dunn, I.S., 1995. Assembly of functional bacteriophage Lambda virions incorporating C-terminal peptide or protein fusions with the major tail protein. J. of mol. biol. 248, 497–506.

Fuh, G., Sidhu, S.S., 2000. Efficient phage display of polypeptides fused to the carboxy-terminus of the M13 gene-3 minor coat protein. FEBS lett. 480, 231-234.

Fischetti, V.A., 2005. Bacteriophage lytic enzymes: novel anti-infectives. Trends in microbiol. 13, 491-496.

Filatova, L.Y., Becker, S.C., Donovan, D.M., Gladilin, A.K., Klyachko, N.L., 2010. LysK, the enzyme lysing *Staphylococcus aureus* cells: specific kinetic features and approaches towards stabilization. Biochim. 92, 507–513.

Filice, G.A., Nyman, J.A., Lexau, C., Lees, C.H., Bockstedt, L.A., Como-Sabetti, K., Lesher, L.J., Lynfield, R., 2010. Excess costs and utilization associated with methicillin resistance for patients with *Staphylococcus aureus* infection. Infect. Control and hosp. epidemiol. 31, 365-373.

Fenton, M., Casey, P.G., Hill, C., Gahan, C.G., Ross, R.P., McAuliffe, O., O'Mahony, J., Maher, F., Coffey, A., 2010. The truncated phage lysin CHAP(k) eliminates *Staphylococcus aureus* in the nares of mice. Bioeng. bugs 1, 404–407.

Gupta, A., Onda, M., Pastan, I., Adhya, S., Chaudhary, V.K., 2003. High-density Functional Display of Proteins on Bacteriophage Lambda. J. of mol. biol. 334, 241-254.

Ho, M., Pastan, I., 2009. Antibody Phage Display 562, 99–113.

Herskowitz, I., 1973. Control of Gene Expression In Bacteriophage Lambda. Annual rev. of genet. 7, 289–324.

Hartman, B.J., Tomasz, A., 1984. Low-affinity penicillin-binding protein associated with beta-lactam resistance in *Staphylococcus aureus*. J. of bacteriol. 158, 513-516.

Hiramatsu, K., 1998. Vancomycin resistance in staphylococci. Drug resist. updates 1, 135-150.

Hiramatsu, K., 2001.Vancomycin-resistant *Staphylococcus aureus* : a new model of antibiotic resistance. The Lancet- Infect. Dis. 1, 147-155.

Hiramatsu, K., Cui, L., Kuroda, M., Ito, T., 2001. The emergence and evolution of methicillin-resistant *Staphylococcus aureus*. Trends in microbiol. 9, 486-493.

Hefti, M.H., Van Vugt-Van der Toorn, C.J., Dixon, R., Vervoort, J., 2001. A novel purification method for histidine-tagged proteins containing a thrombin cleavage site. Anal. biochem. 295, 180–185.

Horgan, M., O'Flynn, G., Garry, J., Cooney, J., Coffey, A., Fitzgerald, G.F., Ross, R.P., McAuliffe, O., 2009. Phage lysin LysK can be truncated to its CHAP domain and retain lytic activity against live antibiotic-resistant staphylococci. Appl. and environ. microbiol. 75, 872-874.

Ho, M., Pastan, I., 2009. Mammalian Cell Display for Antibody Engineering. Methods mol. biol. 525, 337-352.

Hayes, S., Gamage, L.N.A., Hayes, C., 2010. Dual expression system for assembling phage lambda display particle (LDP) vaccine to porcine Circovirus 2 (PCV2). Vaccine 28, 6789-6799.

Ito, T., Katayama, Y., Hiramatsu, K., 1999. Cloning and Nucleotide Sequence Determination of the Entire mec DNA of Pre-Methicillin-Resistant *Staphylococcus aureus* N315 Antimicrob. agents and chemother. 43, 1449.

Knox, R., 1961. Correspondence. British Med. J. 125-126.

Kiedrowski, M.R., Horswill, A.R., 2011. New approaches for treating staphylococcal biofilm infections. Ann. of the New York Acad. of Sci. 1241, 104-121.

Kluytmans, J., van Belkum, A., Verbrugh, H., 1997. Nasal carriage of *Staphylococcus aureus*: epidemiology, underlying mechanisms, and associated risks. Clin. Microbiol. rev. 10, 505-520.

Kondo, A., Ueda, M., 2004. Yeast cell-surface display--applications of molecular display. Appl. microbiol. and biotechnol. 64, 28–40.

Lederberg, E.M., 1951. Lysogenicity in *E. coli* K-12. Genet. 36:560.

Love, C.A., Lilley, P.E., Dixon, N.E., 1996. Stable high-copy-number bacteriophage λ promoter vectors for overproduction of proteins in *Escherichia coli*. Gene 176, 49–53.

Lowy, F., 1998. *Staphylococcus aureus* Infections. The N. Engl. J. of Med. 339, 520-532.

Lowy, F.D., 2003. Antimicrobial resistance : the example of *Staphylococcus aureus*. J. of Clin. Investig. 111, 1265-1273.

Lee, S.Y., Choi, J.H., Xu, Z., 2003. Microbial cell-surface display. Trends in biotechnology 21, 45–52.

Loessner, M.J., 2005. Bacteriophage endolysins--current state of research and applications. Curr. opin. in microbiol. 8, 480-487.

McCafferty, J., Jackson, R.H., Chiswell, D.J., 1991. Phage-enzymes: expression and affinity chromatography of functional alkaline phosphatase on the surface of bacteriophage. Protein eng. 4, 955-961.

Maruyama, I.N., Maruyama, H.I., Brenner, S., 1994. foo: A Phage Vector for the Expression of Foreign Proteins. Proc. of the Natl. of Sci. 91, 8273–8277.

Mikawa, Y.G., Maruyama, I.N., Brenner, S., 1996. Surface display of proteins on bacteriophage Lambda heads. J. of mol. biol. 262, 21-30.

Mattiacio, J., Walter, S., Brewer, M., Domm, W., Friedman, A.E., Dewhurst, S., 2011. Dense display of HIV-1 envelope spikes on the lambda phage scaffold does not result in the generation of improved antibody responses to HIV-1 Env. Vaccine 29, 2637–2647.

Manning, A.J., Kuehn, M.J., 2011. Contribution of bacterial outer membrane vesicles to innate bacterial defense. BMC microbiol. 11, 258.

Nicastro, J., Sheldon, K., El-Zarkout, F. A, Sokolenko, S., Aucoin, M.G., Slavcev, R., 2013. Construction and analysis of a genetically tuneable lytic phage display system. Appl. microbiol. and biotechnol. DOI 10.1007/s00253-013-4898-6

Nicastro, J., Sheldon, K., Slavcev, R., 2013. Bacteriophage λ Display Technology: A Mini Review of Development and Application. In press.

Navarre, W.W., Schneewind, O., 1999. Surface Proteins of Gram-Positive Bacteria and Mechanisms of Their Targeting to the Cell Wall Envelope. Microbiol. and mol. biol. rev. 63, 174–229.

O'Flaherty, S., Coffey, A., Edwards, R., Meaney, W., Ross, R.P. 2004. Genome of Staphylococcal Phage K: A New Lineage of Myoviridae Infecting Gram-Positive Bacteria with a Low G + C Content. J. of bacteriol. 186, 2862.

O'Flaherty, S., Ross, R.P., Meaney, W., Fitzgerald, G.F., Coffey, A., Elbreki, M.F., 2005. Potential of the Polyvalent Anti- Staphylococcus Bacteriophage K for Control of Antibiotic-Resistant Staphylococci from Hospitals. Appl. and environ. microbiol. 71, 1836-1842.

O'Flaherty, S., Coffey, A., Meaney, W., Fitzgerald, G.F., Ross, R.P., 2005. The Recombinant Phage Lysin LysK Has a Broad Spectrum of Lytic Activity against Clinically Relevant Staphylococci, Including Methicillin-Resistant *Staphylococcus aureus*. J. of Bacteriol. 187, 7161-716.

Pavoni, E., Vaccaro, P., D Alessio, V., De Santis, R., Minenkova, O., 2013. Simultaneous display of two large proteins on the head and tail of bacteriophage Lambda. BMC biotechnol. 13, 79.

Petty, N.K., Evans, T.J., Fineran, P.C., Salmond, G.P.C., 2007. Biotechnological exploitation of bacteriophage research. Trends in biotechnol. 25, 7-15.

Ralston, D.J., Lieberman, M., Baer, B., Krueger, A.P., 1957. Staphylococcal virolysin, a phage-induced lysin; its differentiation from the autolysis of normal cells. The J. of gen. physiol. 40, 791-807.

Rodenburg, C.M., Mernaugh, R., Bilbao, G., Khazaeli, M.B., 1998. Production of a single chain anti-CEA antibody from the hybridoma cell line T84.66 using a modified colony-lift selection procedure to detect antigen-positive ScFv bacterial clones. Hybrid 17, 1-8.

Public Health Agency of Canada, 2009. Results of the Surveillance of Methicillin Resistant *Staphylococcus aureus*, a project of the Canadian Nosocomial Infection Surveillance Program (CNISP).

Ruef, C., 2004. Epidemiology and clinical impact of glycopeptide resistance in *Staphylococcus aureus.* Infect. 32, 315–327.

Rodríguez-Rubio, L., Martínez, B., Donovan, D.M., Rodríguez, A., García, P., 2012. Bacteriophage virion-associated peptidoglycan hydrolases: potential new enzybiotics. Crit. rev. in microbiol. 1–8.

Schmelcher, M., Powell, A.M., Becker, S.C., Camp, M.J., Donovan, D.M., 2012. Chimeric phage lysins act synergistically with lysostaphin to kill mastitis-causing Staphylococcus aureus in murine mammary glands. Appl. environ. microbiol. 78, 2297–305.

Schindler, C.A., Schuhardt, V.T., 1964. Lysostaphin:A New Bacteriolytic agent for the Staphylococcus. Proc. of the Natl. Acad. of Sci. 447, 414–421.

Sonstein, S.A., Hammel, J.M., Bondi, A., 1971. Staphylococcal bacteriophage-associated lysin: a lytic agent active against *Staphylococcus aureus*. J. of bacteriol. 107, 499-504.

Sternberg, N., Weisberg, R., 1977. Packaging of coliphage Lambda DNA. II. The role of the gene D protein. J. of mol. biol. 117, 733-759.

Skinner, D., Keefer, C.S. 1941.Significance of Bacteremia caused by *Staphylococcus aureus*. Arch. Intern. Med. 68, 851-875.

Sharma, S.K., Evans, D.B., Vosters, A.F., Chattopadhyay, D., Hoogerheide, J.G., Campbell, C.M., 1992. Immobilized Metal Affinity Chromatography of Bacterially Expressed Proteins Engineered to Contain an Alternating-Histidine Domain. A Companion to Methods in Enzym. 4, 57-67.

Sternberg, N., Hoess, R.H., 1995. Display of peptides and proteins on the surface of bacteriophage Lambda. Proc. of the Natl. Acad. of Sci. of the U. S. A. 92, 1609-1613.

Shoji, M., Cui, L., Iizuka, R., Komoto, A., Neoh, H., Watanabe, Y., Hishinuma, T., Hiramatsu, K., 2011. *walK* and *clpP* mutations confer reduced vancomycin susceptibility in *Staphylococcus aureus*. Antimicrob. agents and chemother. 55, 3870–3881.

Szweda, P., Schielmann, M., Kotlowski, R., Gorczyca, G., Zalewska, M., Milewski, S., 2012. Peptidoglycan hydrolases-potential weapons against *Staphylococcus aureus*. Appl. microbiol. and biotechnol. 96, 1157–1174.

Strauss, A., Gotz, F., 1996. In vivo immobilization of enzymatically active polypeptides on the cell surface of *Staphylococcus carnosus*. Mol. Microbiol. 21, 491–500.

Vílchez, S., Jacoby, J., Ellar, D.J., 2004. Display of Biologically Functional Insecticidal Toxin on the Surface of Phage. Appl. and environ. microbiol. 70, 6587-6594.

Vaccaro, P., Pavoni, E., Monteriù, G., Andrea, P., Felici, F., Minenkova, O., 2006. Efficient display of scFv antibodies on bacteriophage Lambda. J. of immunol. methods 310, 149-158.

Valdez-Cruz, N. A, Caspeta, L., Pérez, N.O., Ramírez, O.T., Trujillo Roldán, M. A, 2010. Production of recombinant proteins in E. coli by the heat inducible expression system based on the phage lambda pL and/or pR promoters. Microb. cell fact. 9, 18.

Van Bloois, E., Winter, R.T., Kolmar, H., Fraaije, M.W., 2011. Decorating microbes: surface display of proteins on Escherichia coli. Trends in biotechnol. 29, 79–86.

Weigel, L.M., Clewell, D.B., Gill, S.R., Clark, N.C., McDougal, L.K., Flannagan, S.E., Kolonay, J.F., Shetty, J., Killgore, G.E., Tenover, F.C., 2003. Genetic analysis of a high-level vancomycin-resistant isolate of *Staphylococcus aureus*. Sci. 302, 1569–1571.

Willats, W.G.T., 2002. Phage display: practicalities and prospects. Plant mol. biol. 50, 837–854.

Yang, F., Forrer, P., Dauter, Z., Conway, J.F., Cheng, N., Cerritelli, M.E., Steven, A. C., Plückthun, A., Wlodawer, A., 2000. Novel fold and capsid-binding properties of the Lambda-phage display platform protein gpD. Nat. struct. biol. 7, 230–237.

Zanghi, C.N., Lankes, H.A., Bradel-Tretheway, B., Wegman, J., Dewhurst, S., 2005. A simple method for displaying recalcitrant proteins on the surface of bacteriophage Lambda. Nucleic acids res. 33, 1-7.